Renewable Resource Based Block Copolymers and Their Self Assembly

MS Thesis Report submitted towards the partial fulfillment of

BS-MS dual degree program

By

Sharada Sarjane

20141038

Under the guidance of

Prof. M. Jayakannan

Indian Institute of Science Education and Research (IISER) Pune

March 2019

CERTIFICATE

This is to certify that this dissertation entitled "**Renewable Resource Based Block Copolymers and Their Self Assembly**" towards the partial fulfilment of the BS-MS dual degree programme at the Indian Institute of Science Education and Research, Pune represents work carried out by "Sharada Kailas Sarjane at IISER Pune" under the supervision of "Prof. M. Jayakannan" during the academic year 2018-2019.

Date: 20/03/2019

Place: IISER, Pune

(Sharada Sarjane)
20141038

Date: 20/3/2019

Place:

(Prof. M. Jayakannan)

DECLARATION

I hereby declare that the matter embodied in the report entitled "**Renewable Resource Based Block Copolymers and Their Self Assembly**" are the results of the work carried out by me at the Department of Chemistry, IISER Pune, under the supervision of Prof. M. Jayakannan and the same has not been submitted elsewhere for any other degree.

Date: 20/03/2019

Place: IISER, Pune

(Sharada Sarjane)
20141038

Date: 20/3/2019

Place:

(Prof. M. Jayakannan)

ACKNOWLEDGEMENTS

I would like to utilize this opportunity to express my sincere gratitude towards my thesis supervisor M. Jayakannan for giving me opportunity to work in his lab and also for his constant encouragement, guidance and support.

I am grateful to my TAC member, Dr. Sandanaraj Britto for his valuable suggestions in the TAC meetings.

I would like to thank Mehak Malhotra for her continuous guidance, help and motivation for keep me going and also for her patience in answering all my doubts.

I am delighted to express my gratitude towards all the IISER faculties for their support in pursuing my dreams at IISER.

I am indebted to all technical staff members Mahesh, Sandeep, Swati, Nitin, Ganesh for making my research easier at IISER.

This journey wouldn’t have been possible without all my present and former lab members, Nilesh, Bhagyashree, Ruma, Sonashree, Dheeraj, Sharafu, Anu, Uttareshvar, Pranav, Khuddus, Rasika, Mishika, Akash, I thank them all for their cooperation, support and guidance.

I am grateful to my parents, sister Geeta and brother Ganesh for their love and support.

--Sharada

CONTENTS

List of figures and Tables

Abstract:

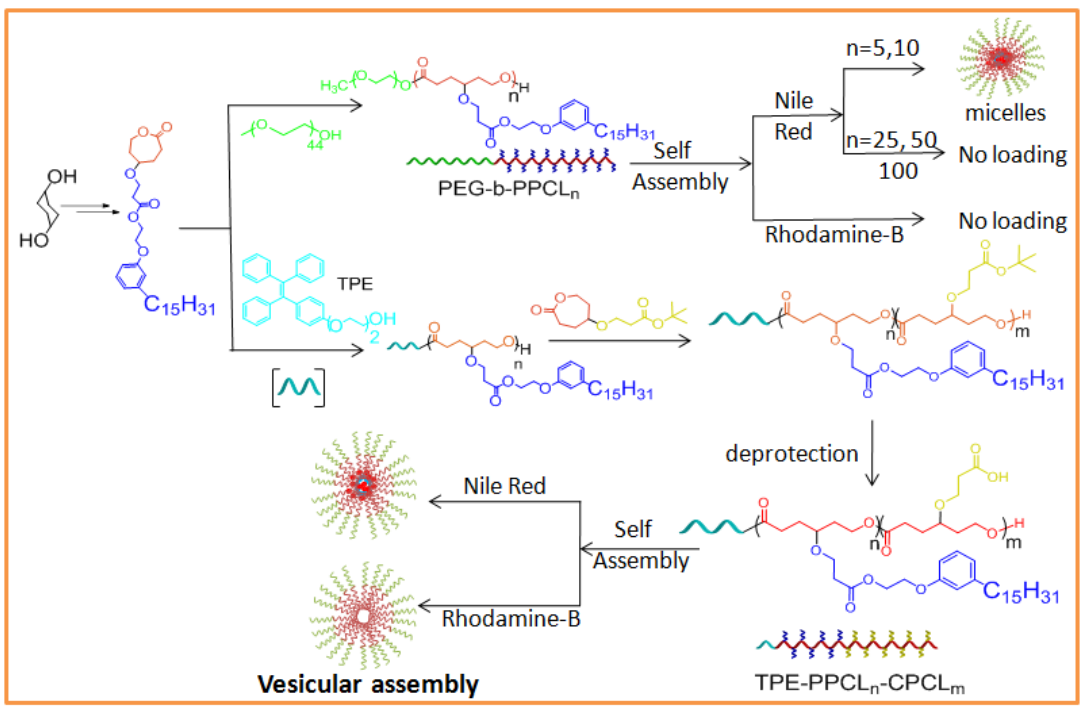

The objective of this thesis is to incorporate the bio-resource based vesicular directing group, pentadecyl phenol (PDP), into caprolactone based block copolymers and see its effect onto the self assemblies of these polymers. For this purpose PDP substituted caprolactone monomer was synthesized, it was further ring opened using PEG as an initiator to get amphiphillic block copolymer, PEG-b-PPCL$_n$ (PPCL-PDP substituted polycaprolactone). Once the repeating units of monomer in a hydrophobic block (PPCL$_n$), necessary for self assembly are optimized, fluorescent tagged polymers (TPE-PPCL$_n$-CPCL$_m$) were synthesized with TPE (tetraphenyl ethene) as an initiator and CPCL (carboxylic substituted polycaprolactone, discussed in introduction) as a hydrophilic block were synthesized and their self assembly was studied. All monomers and polymers were characterized using ^{1}H NMR, ^{13}C NMR and FT-IR. Thermal stability and semicrystallinity of these polymers was checked using thermogravimetric analysis and Differential Scanning Calorimetry respectively and it is found that all polymers are semicrystalline and thermally stable upto 250 °C. Hydrophobicity of all the polymers was analyzed from Water Contact Angle. It was found that, PEG-b-PPCLn forms micellar self assemblies whereas TPE polymers produce vesicular assemblies of around 200 nm in water. These nano-assemblies were further characterized using DLS and FE-SEM. Drug loading capabilities of these polymers was checked using dialysis method of self assembly. Cell viability assay of drug loaded nano-carriers suggested that they are cytotoxic to the cancer cells and cellular uptake of these nano-assemblies was confirmed by confocal laser scanning microscopy. Photo-physical studies of TPE-PPCL$_n$-CPCL$_m$ were performed and it was found that TPE gives aggregation induced emission upon self assembly and these self assemblies also show FRET upon encapsulation of dye such as Rhodamine-B. Cellular uptake studies of these polymers are under progress.

Introduction:

1.1 Why Nano-assemblies for drug delivery:

The medical science has gathered a lot of insight into diagnosis and treatment of cancer or tumor, but they still face the challenge of efficient delivery of therapeutic drugs in a site specific and timely manner. Regular drug delivery systems have limitations such as maintaining the drug concentration in a therapeutic window, non targeted delivery and some of them are shown diagrammatically in Figure 1.1[1,2] .

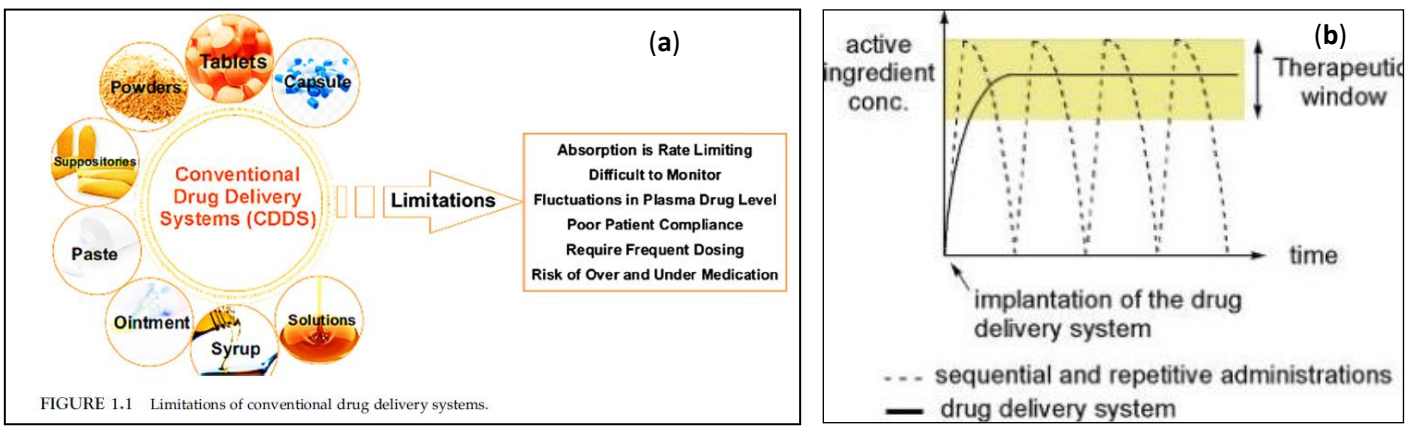

Figure 1.1: (a) Limitations of CDDS [1] (b) Change in plasma drug concentration using CDDS and CRDDS [2]

These above challenges can be tackled to some extent by using block copolymer (section 1.2) based nano-assemblies for encapsulation and delivery of drug in a spacio-temporal way, it also enable us to release drug in controlled way (Figure 1.1(b)), such that the drug concentration remains in the therapeutic window. Tumor tissues are characterized by vascular abnormalities, poor lymphatic drainage weak acidity, over expression of some receptors, enzymes, abnormal temperature, hypoxia etc and one can exploit these properties to synthesize smart polymer based assemblies, which can respond to these stimuli and enables the programmable delivery of encapsulated drug. And not only this, these assemblies can also be responsive to intracellular pH gradient and redox and H_2O_2 gradient within cell organelles, upon cellular uptake. Figure 1.2 depicts the fate of block copolymer based nano-assemblies once they enter into the circulatory system and it also depicts the characteristics of tumor tissue, which we can exploit to design drug delivery systems [3]

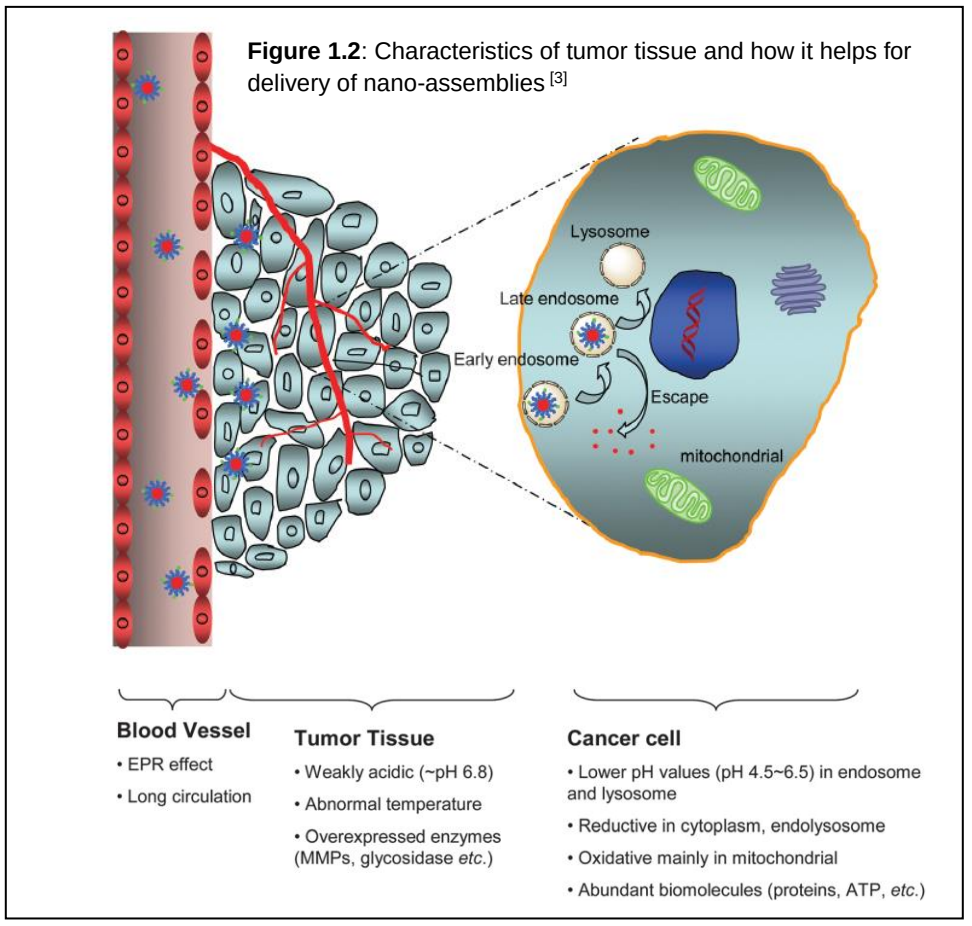

1.2 Block copolymers:

Block copolymers are the copolymers in which single polymer contains chemically distinct blocks, which are synthesized from sequential addition of different monomer units or by coupling of active polymer chain ends. One can synthesize block copolymer with various chemical compositions, architecture (linear, brushed, star shaped, centipede etc) or topology [4] , Cheng et al have used the azide-alkyne click reaction of PLA with PTX and PEG containing an azide functional group (scheme 1.1) to synthesize biodegradable brushed polymers for drug delivery [5].

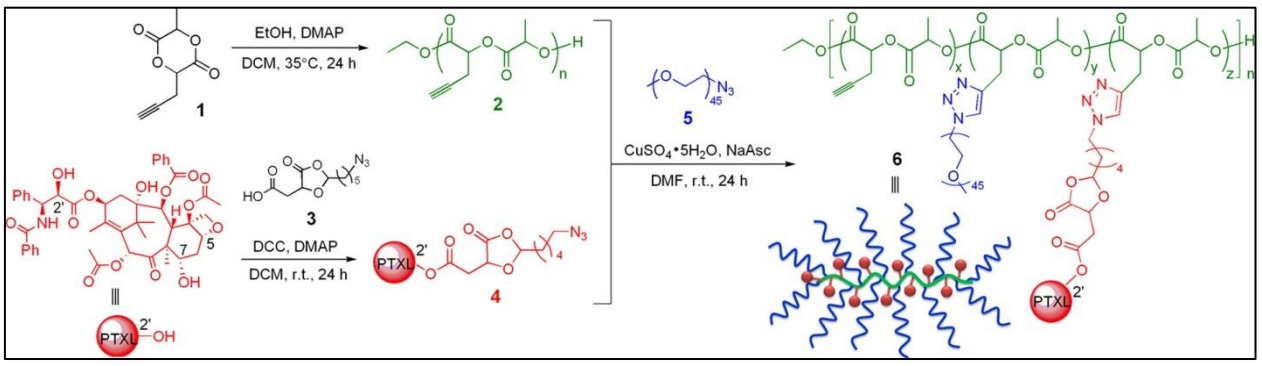

Scheme 1.1: Synthesis scheme of brushed polymers (**6**) for drug delivery using click chemistry [5]

Synthesis of these block copolymers can be achieved through various controlled polymerization techniques such as ROP, ATRP, RAFT, etc. to get polymers with narrow polydispersity index and desired molecular weight [6]. Hong et. al have synthesized PHPMA-*b*-PNIPAAm block copolymers using RAFT polymerization (scheme 1.2), these are biotinylated and thermoresponsive amphiphillic polymers, which has application in targeted drug delivery [7]. Block copolymers not only used in drug delivery, but they also have diversity of application in soft lithography and mesoporous material synthesis [4]

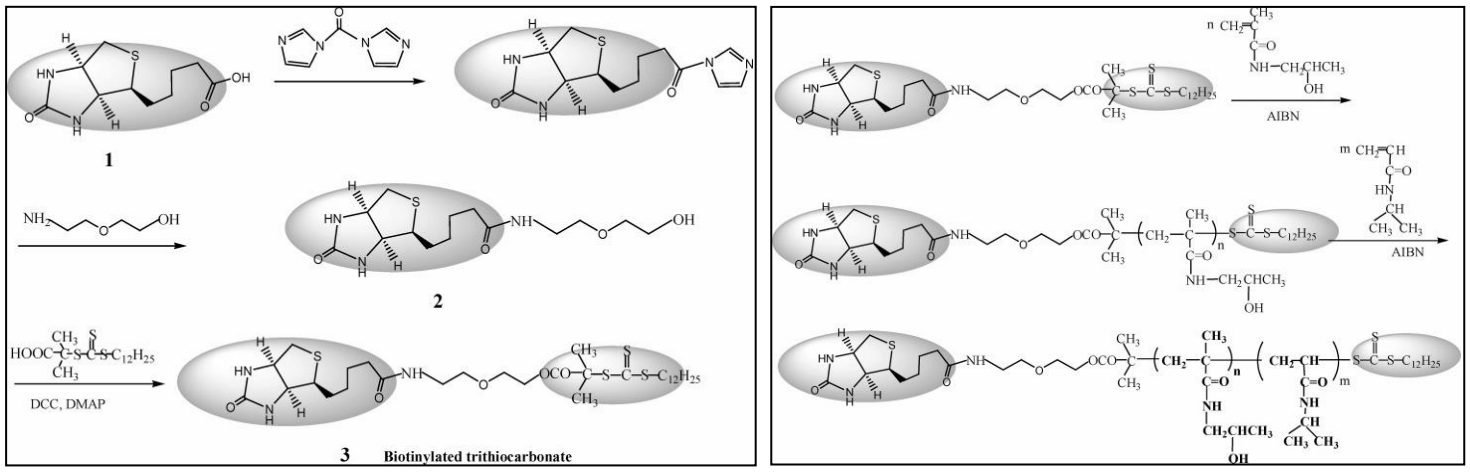

Scheme 1.2: Synthesis of RAFT agent (**3**) and PHPMA-*b*-PNIPAAm block copolymers using RAFT polymerization [7]

Biodegardability and biocompatibility:

Block copolymers are highly exploited in the field of drug delivery and for it to be a better candidate for drug delivery they have to be biocompatible (non-toxic and non immunogenic), which includes polyethylene glycol (PEG), FDA approved polyesters and polyacrylamides, moreover they also have to be biodegradable (degrades into products that can be excreted, metabolized, resorbed), which includes poly(ε-caprolactone)s (PCL), poly(lactic acid)s (PLAs) and poly(glycolic acid)s (PGAs) [8] .

1.3 Self Assembly of block copolymers:

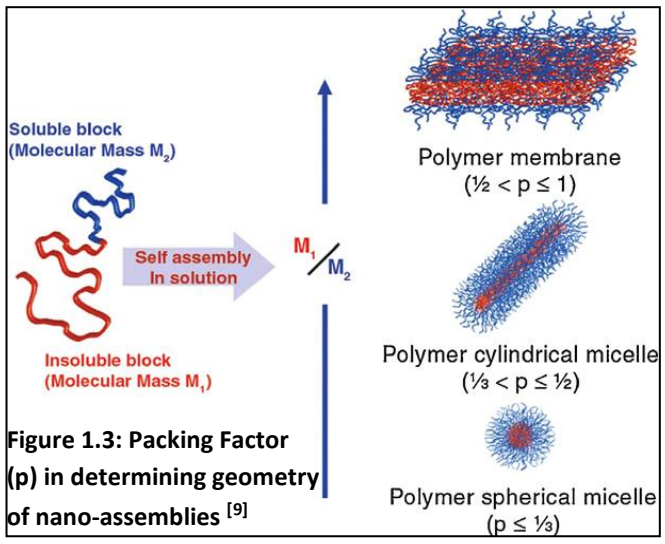

Figure 1.3: Packing Factor (p) in determining geometry of nano-assemblies [9]

Amphiphillic block copolymer consisting of hydrophilic and hydrophobic parts are highly exploited in drug delivery application because they can self assemble to form various nanostructures such as vesicle, micelle, cylindrical micelle, rods etc, which encapsulate drugs and increase the efficiency of its delivery. One can determine the morphologies of these nanostructures by using packing parameter (Figure 1.3) that is **p = v/al** where **v** is volume of hydrophobic part, **a** is the area of hydrophilic head and **l** is the length of hydrophobic tail. Spherical micelles are formed when p<1/3, for cylindrical micelles it is 1/3<p<1/2 and for polymer membranes or polymerosome like vesicle it is ½≤p≤1. Self assembly not only depends on this parameter but also on chemical composition and architecture of the polymer. [4,9]

Morphological transitions (from sphere to cylinder to lamellae) can be seen in polymeric assembly, based on many factors, main deciding factors are interfacial energy between two blocks (enthalpy contribution) and chain stretching (entropic factor). As the effective volume fraction of B decreases upon increase in f_A (volume fraction of A), polymer chains take on new arrangements to reduce their stretching and this lead to the formation of less curved interfaces and thus lead to morphological transitions (Figure 1.4) [10,11].

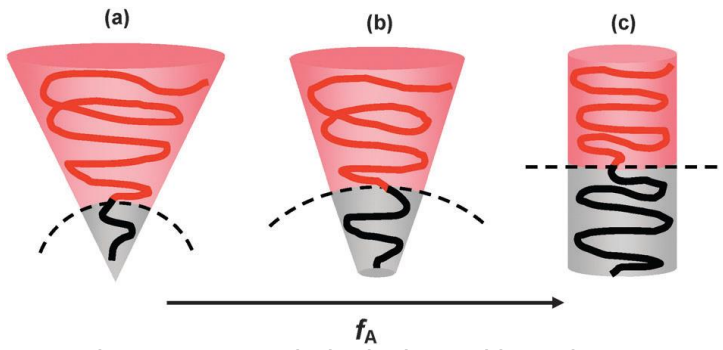

Figure 1.4: morphological transitions due to increase in *fa* [10]

In case of micelles hydrophobic part helps in encapsulating the drug and hydrophilic part facilitates the solubility of the nanocarrier in the aqueous medium. Heterogeneous behavior of tumors adds the complexity of multi drug resistance (MDR) in cancer therapy, one way to address this complexity to certain extent is to use polymer vesicles (drug carrier), which are capable of loading multiple drugs (hydrophilic and hydrophilic both) allow us to overcome MDR to certain extent.

1.4 Polycaprolactone:

These are biodegradable and semicrystalline aliphatic polyesters, which consist of hexanoate repeating units. It has solubility in chloroform, dichloromethane, tetrachloromethane, benzene, toluene and it also shows partial solubility in acetone, ethyl acetate acetonitrile etc. Degree of crystallinity and molecular weight decide its mechanical, thermal and physical properties and also the biodegradation [12].

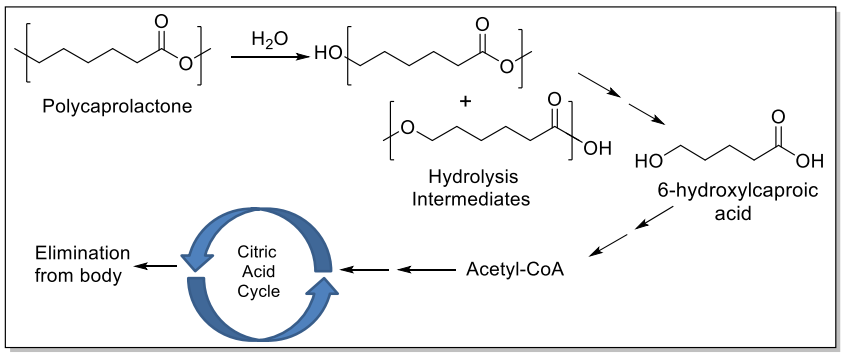

Scheme 1.3: hydrolytic degradation of PCL [13]

It can take several months to years for biodegradation, which depend on factors such as degradation condition and degree of crystallinity of the polymer. Here amorphous phase is degraded first and then the crystalline phase, carboxylic acid generated during its hydrolysis (Scheme 1.3) helps in the

autocatalysis, although it can be degraded enzymatically in the environment, it can't be degraded enzymatically in the body [12, 13].

Monomer Synthesis:

- It is one of the intermediary product in oxidation pathway of cyclohexanol in microbes (Scheme 1.4(a)).
- Industrially it is synthesized by oxidation of cyclohexanone by peracetic acid (Scheme 1.4(b)).

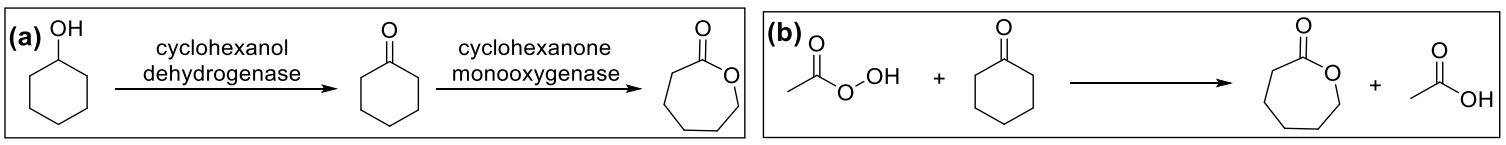

Scheme 1.4: Microbial (a) and industrial synthesis (b) of caprolactone [12]

There are two ways by which polycaprolactone can be synthesized one is polycondensation and other is ring opening polymerization (ROP, next section). Polycondensation yields polymers with high polydispersity and lower molecular weight, whereas ROP gives polymers with narrow PDI and higher molecular weight and this is the reason why ROP is the most widely used method of synthesis [11].

Properties such as mixing with other polymers, monomer synthesis based on renewable resources, compatibility with biological systems and controlled degradation contributes to the wide applicability of these polymers. To further increase the versatility of PCL one can substitute the caprolactone or synthetically modify the PCL to produce functionalized PCL and this synthetic flexibility of PCL among all other aliphatic biodegradable polyesters such as PLA and PGA makes PCL more dominated in bio-application [8]. Functionalization of PCL (one of the example is shown in Scheme 1.5) modifies the polymer in various ways such as increasing the drug loading efficiency or crystallinity of the polymer etc. Bapurao *et al.* designed novel monomer t-butyl-3-((7-oxooxepan-4-yl)oxy)-propanoate (Scheme 1.5(a)), which upon ROP followed by deprotection generates carboxylic substituted PCL, which was further reacted with cisplatin to synthesize cisplatin stitched polymers (Scheme 1.5(b)) achieving 16 wt% loading [15]. This example shows that the cisplatin, can be delivered in efficient way by functionalization of PCL.

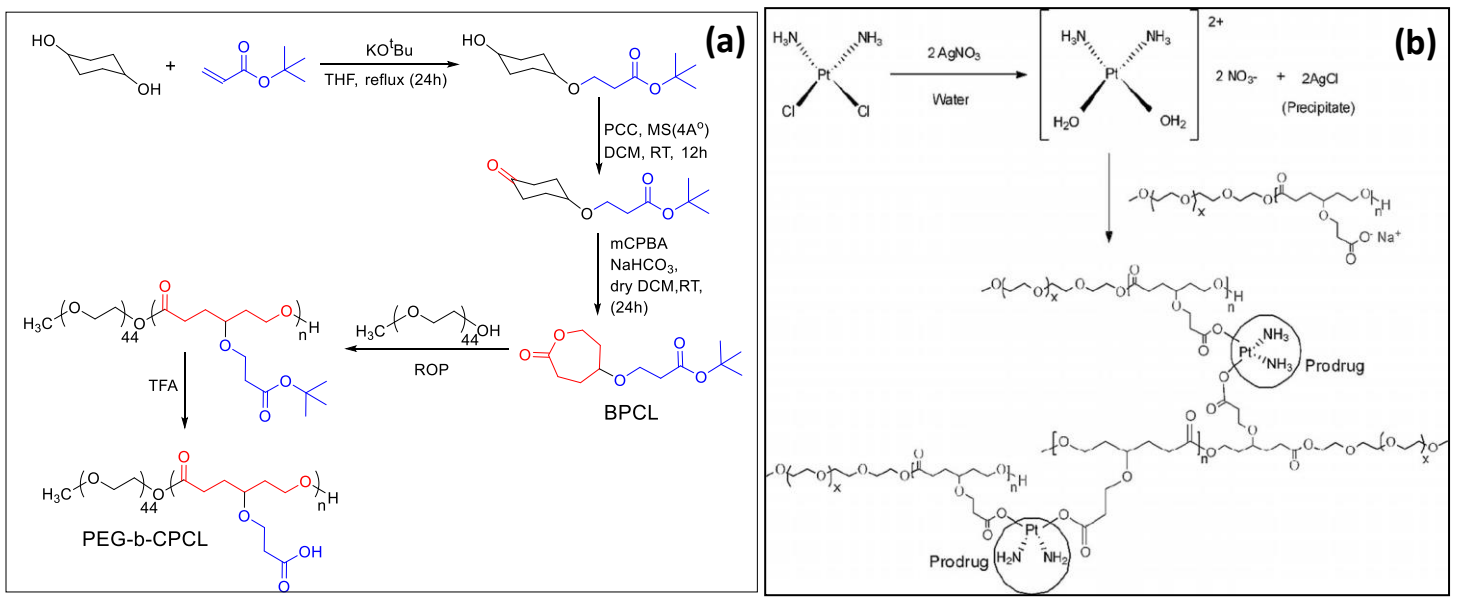

Scheme 1.5: (a) Synthesis of PEG-b-CPCL polymer [16] (b) Cisplatin stitching onto the polymer [15]

1.5 Ring Opening Polymerization:

It is among one of the method of polymerization, which comes under living polymerization where process of termination of chain and chain transfer are suppressed or eliminated. Here chain initiation is faster and almost all the active moieties are generated in the beginning itself (Figure 1.5(a)), moreover rate of propagation is slower than initiation and all the chains grow at constant rate, whereas in non living polymerization chain initiation is not a instantaneous process and all chain does not grow at constant rate (Figure 1.5(b)), and these factors contribute to yield polymers with narrow polydispersity and uniform molecular weight (Figure 1.5(c)).

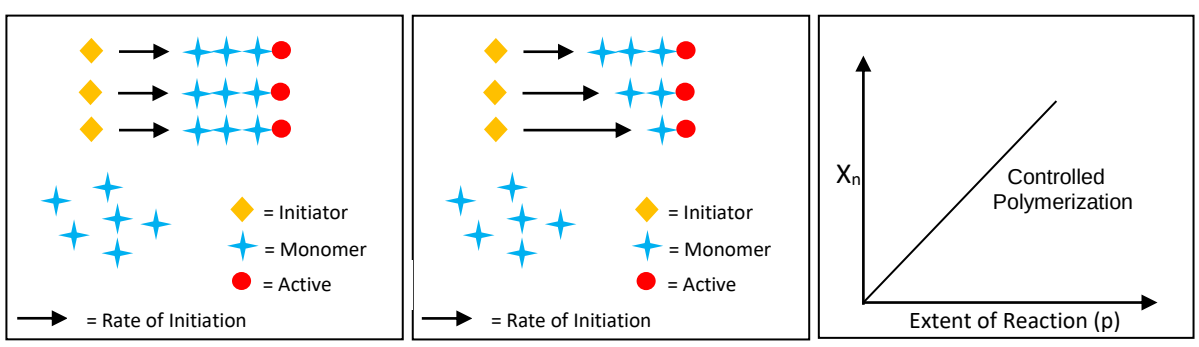

Figure 1.5: (a) Living polymerization, (b) Non-living polymerization, (C) Controlled nature of ROP

In ROP ring strain is the driving force for the polymerization to occur and not only this, temperature condition is also one of the deciding factors for the rate of polymerization. There are number of mechanisms such as anionic, cationic, coordination insertion and monomer activated ROP (Scheme 1.8) in which the polymerization can proceed. Cationic ROP follows bimolecular nucleophilic substitution mechanism, where carbonyl oxygen of monomer attacks the cationic species to generate the active species. Anionic ROP proceeds via generation of active alkoxide species, which is generated by attack of cationic species at carbonyl carbon of monomer. In monomer activated ROP catalyst attacks the monomer and activates it, activated monomer further attacks the polymer chain end to carry out the reaction. Coordination insertion mechanism involves coordianation of catalyst and monomer and then insertion of monomer into metal oxygen bond, metal remains attached to the chain throughout the propagation, catalyst such as Lithium diisopropyl (LDA), cyclopentadienyl sodium, Triethyl aluminium, tin (II) octoate, etc. Sometimes we may get polymers with undesired molecular weight due to some of the side reactions, which involves intra molecular transesterification, ring elimination and counterion collapse [12].

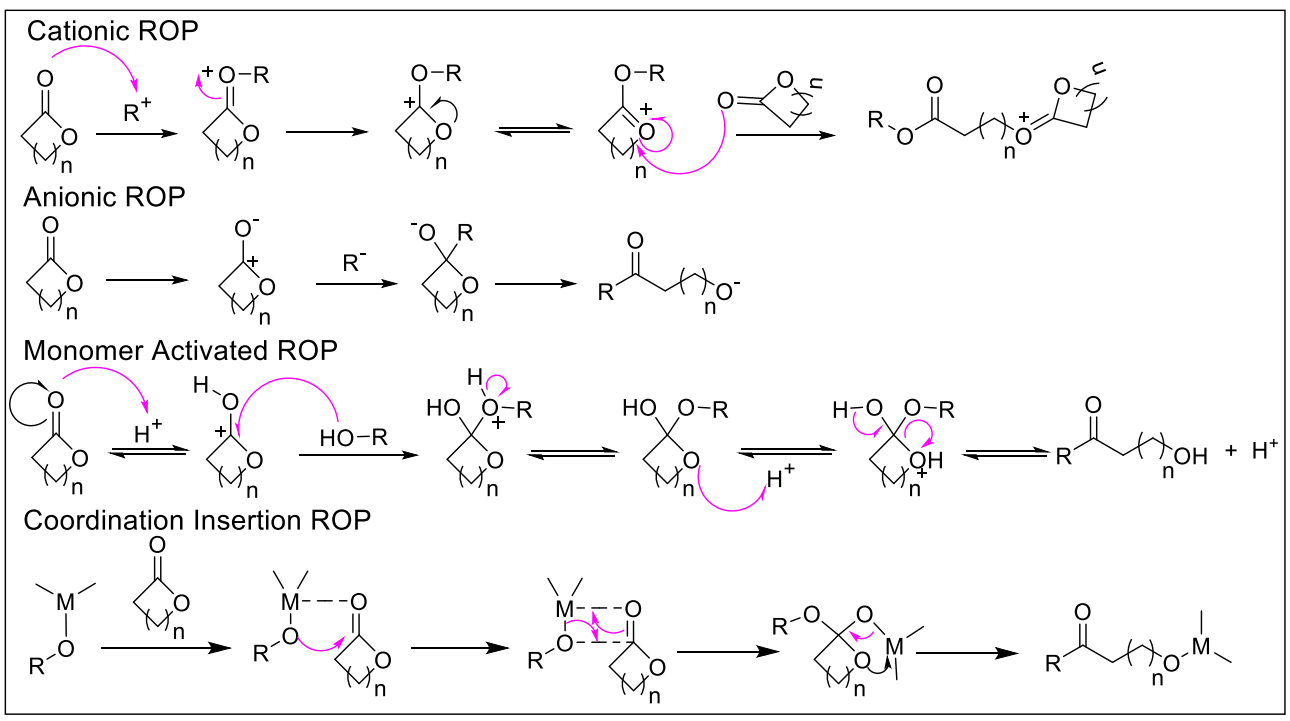

Scheme 1.6: Different mechanisms of ROP

1.6 Inspiration for the thesis

A. Vesicular Assemblies using PCL**:**

It is known that PEG-b-PCL forms micellar assemblies and are studied for drug delivery application but they can't form vesicular morphologies, which increase the drug loading efficiency and also enable us to load more than one drug which in turn can help in tackling the problem of MDR, so synthetic modification in PCL are required to obtain the vesicular nano-assemblies and taking inspiration from this Bapurao *et al.* (Figure 1.6(a)) has designed amphiphillic block copolymer consisting of carboxylic substituted polycaprolactone (CPCL) as a one block and PEG as another block, using ROP and found that they self assemble into vesicular morphologies. One more added advantage of using CPCL is that these vesicles are pH responsive that is they are stable at acidic pH and degrades at neutral pH, these factors made them suitable for targeted oral drug delivery carrier for colon cancer treatment [16].

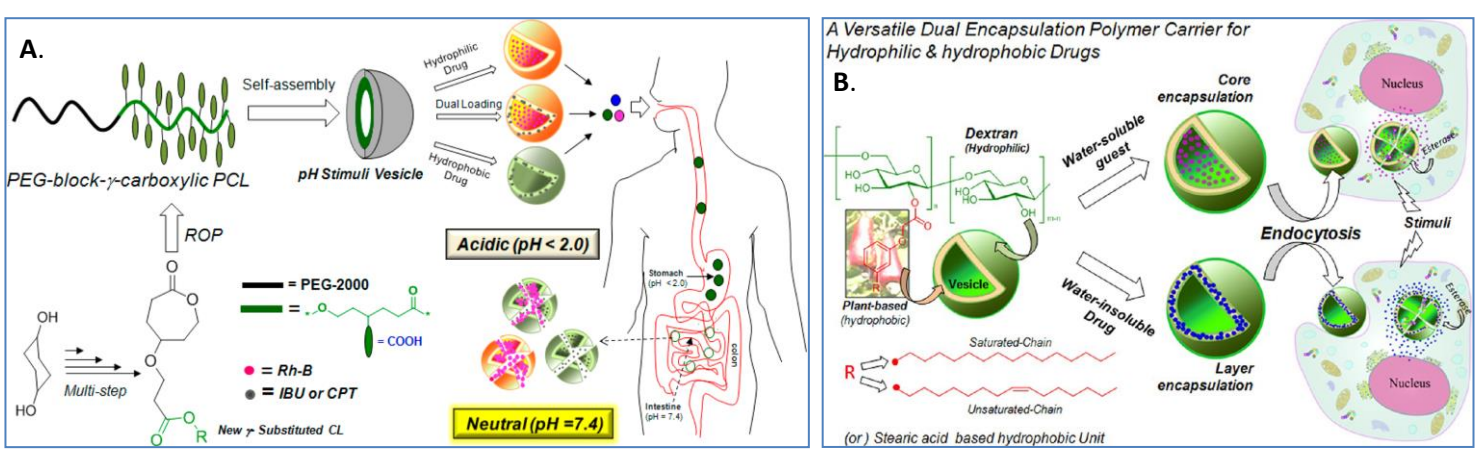

Figure 1.6: (**A.**) Block copolymer based vesicles [16] (**B.**) PDP based vesicular assemblies [17]

B. PDP as a vesicle directing group**:** PDP shows a property of interdegitization, which helps in a formation of bilayer like structure required for vesicular assembly. [3, 4] Pramod *et al.* (Figure 1.6(b)) have shown that incorporation of optimized % of PDP in a dextran based amphiphillic polymer helps the polymer to form vesicular nano-assemblies [17].

Taking inspiration from these ideas we thought of combining these two concepts that is to incorporate PDP substitution in block copolymer and study the self assembled morphologies of these block copolymer. Thus the aim of this thesis is to synthesize amphiphillic block copolymer consisting of PDP substituted caprolactone units as a hydrophobic part and polyethylene glycol (PEG-2K) as a hydrophillic part, Ring Opening Polymerization technique was used to get polymers with controlled molecular weight and specific architecture. Further we are interested in finding out what morphologies these polymers can self assemble into?

2. Experimental methods

2.1 Materials: 1,4-Cyclohexanediol, tert-butyl acrylate, potassium tert-butoxide, pyridinium chlorochromate (PCC), molecular sieves (4Å), Trifluoroacetic acid (TFA), meta-chloroperoxybenzoic acid (mCPBA), N,N'-Dicyclohexylcarbodiimide (DCC), Dimethylaminopyridine (DMAP), 2-bromo ethanol, benzophenone, 4-Hydroxybenzophenone, tin(II) 2-ethylhexanoate ($Sn(oct)_2$), Caprolactone (CL), pentadecylphenol and nile red, doxorubicin (DOX), Rhodamine-B were purchased from Sigma Aldrich. Na_2SO_4, $NaHCO_3$, $Na_2S_2O_3$, Na_2SO_4, NaOH, HCl, potassium carbonate and potassium iodide were purchased locally.

Solvents: Acetonitrile, diethyl ether, Tetrahydrofuran (THF), methanol, petroleum ether, ethyl acetate and Dichloromethane (DCM) were distilled and purified prior to use.

2.2 Methods: The synthesis of the entire molecules was confirmed by ^{1}H and ^{13}C NMR spectra, which were recorded using 400 MHz and 100MHz JEOL NMR spectrophotometer respectively. All NMR spectra were recorded in $CDCl_3$ or DMSO-d_6 solvents having TMS as internal standard. The mass of monomer was analyzed using HRMS-ESI-Q-time of flight LCMS. Viscotech RI and Viscotech UV/Vis detector were used in Gel Permeation Chromatographic (GPC) analysis, which was performed in Tetrahydrofuran (THF) using polystyrene standards. Thermal stability analysis of the polymers was done using PerkinElmer thermal analyzer at a heating rate of 10 °C/min in nitrogen atmosphere. Thermal properties of all polymers were analyzed using TA Q20 Differential Scanning Calorimeter. All the polymers were heated to melt before recording in order to remove previous thermal history. Polymers were heated and cooled at a rate of 10 °C/min in nitrogen atmosphere. Dynamic light scattering (DLS) was performed using Nano ZS-90 apparatus, 633 nm red laser (at 90° angle) from Malvern Instruments was used for these measurements. Absorption studies were performed by using Perkin-Elmer Lambda 45 UV-Visible spectrophotometer. Fluorescence spectra for all the flurophore were recorded using SPEX Fluorolog HORIBA JOBIN VYON fluorescence, where 150 W Xe lamp was used as the source of excitation at room temperature. Images of water drop on polymer surface were captured using DIGIDROP instrument GBX model and imageJ software was used to analyze these images to get water contact angle. FESEM images of drop casted samples on silicon wafers were taken by using Zeiss Ultra Plus scanning electron microscope. MCF 7 cells were incubated with drug loaded polymers and Confocal images were captured by using LSM710 microscope.

2.3 Multistep synthesis of PDP substituted caprolactone:

1. Synthesis of tert-butyl 3-((4-hydroxycyclohexyl)oxy)propanoate (**1**): Cyclohexane-1,4-diol (25g, 215.5mmol) was dissolved in dry THF (350 ml) under nitrogen. Catalytic amount of potassium t-butoxide was added to it and this mixture was refluxed for 30 min. t-Butyl acrylate (22g, 172.4 mmol) dissolved in dry THF (50 ml) was added to the above mixture in a dropwise manner using dropping funnel at room temperature and the reaction mixture was refluxed for 24 h. THF was evaporated using rotavapor and unreacted cyclohexanediol was removed by precipitation in DCM. DCM was evaporated to get the crude product. Further purification was done using column chromatography to get product (**1**), for this ethyl acetate and hexane (3:20 v/v) was used as an eluent. Yield = 16g (38 %)

   ^{1}H NMR (400 MHz, $CDCl_3$) δ ppm: 3.66 (m, 3H, O-CH_2- and O-CH), 3.36-3.37 (m, 1H, CH-OH), 2.44 (t, 2H, -CH_2CO-),1.97-1.79(m, 4H, -CH_2-),1.63(m, 2H,-CH_2-),1.43 (s, 9H, - C(CH_3)), 1.3 (m, 2H, -CH_2-).

   ^{13}C NMR (100 MHz, $CDCl_3$) δ ppm: 171.09, 80.42, 69.51, 63.95, 63.52, 32.53, 30.34, 29.18, and 27.43.

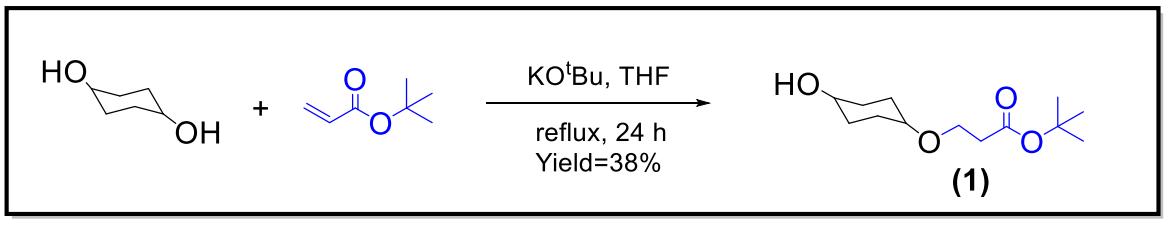

Scheme 2.1

2. Synthesis of tert-butyl 3-((4-oxocyclohexyl)oxy)propanoate (**2**): Compound (**1**) (16g, 65.6 mmol) was dissolved in dry DCM (320 ml), some amount of molecular sieves (4 Å) were added into it and the mixture was stirred for 10 min under nitrogen. PCC (28.3g, 131.1mmol) was added into it and reaction mixture was stirred for 12 h. Reaction mixture was filtered to remove molecular sieves and extracted crude product was further purified by passing through silica column using ethyl acetate and hexane (1:10 V/V) as an eluent to get product (**2**). Yield = 14g (88 %). ^{1}H NMR (400 MHz, $CDCl_3$) δ ppm: 3.72 (m, 3H, O-CH_2- and O-CH), 2.58 (m, 2H, -CH_2CO-), 2.49 (t, 2H, -CH_2-), 2.24 (m, 2H, -CH_2-), 2.04 (m, 2H, -CH_2-), 1.88 (m, 2H, -CH_2-) 1.42 (s, 9H, - C(CH_3)). ^{13}C NMR (100 MHz, $CDCl_3$) δ ppm: 211.41, 170.98, 80.52, 72.73, 64.01, 37.01, 36.54, 30.41, 20.03.

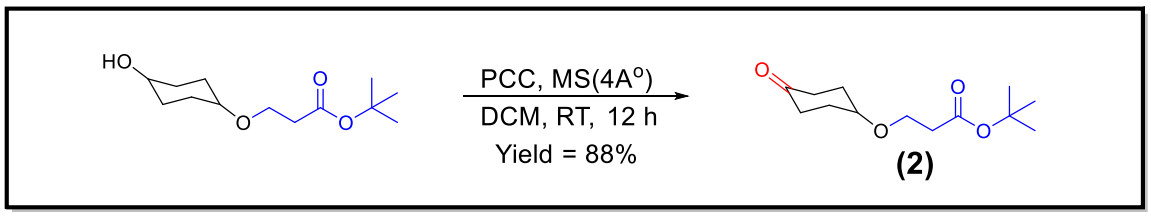

Scheme 2.2

3. Synthesis of 3-((4-oxocyclohexyl)oxy)propanoic acid (**3**): Compound (**2**) (5g, 20.6mmol) was dissolved in DCM and TFA (16.48g, 144.6mmol) was slowly added to it and reaction mixture was stirred for 4 h at room temperature. DCM and TFA was evaporated using rotavapor and further purification was done by passing the crude product through silica column using ethyl acetate and hexane (1:20 v/v) to get product (**3**). Yield=3.3g(89%). ^{1}H NMR (400 MHz, $CDCl_3$) δ ppm: 3.76 (m, 3H, O-CH_2- and O-CH), 2.66 (t, 2H, -CH_2-), 2.58 (m, 2H, -CH_2CO), 2.26 (m, 2H, -CH_2-), 2.1 (m, 2H, -CH_2-), 1.91 (m, 2H, -CH_2-).^{13}CNMR (100 MHz, $CDCl_3$) δ ppm: 212.75, 177.43, 72.99, 63.42, 37.01,35.19, 30.37.

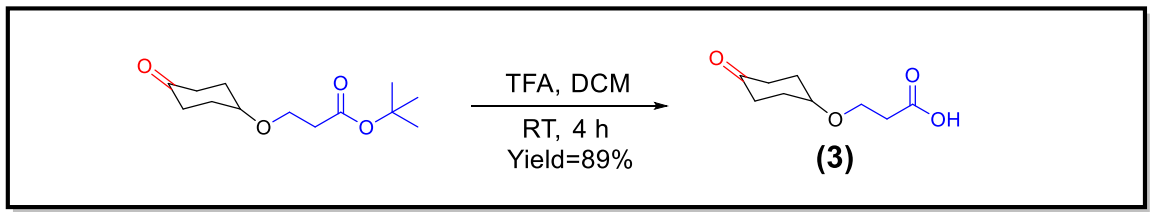

Scheme 2.3

4. Synthesis of 2-(3-pentadecylphenoxy)ethan-1-0l (**4**): 3-Pentadecylphenol (12g, 39.4mmol) was dissolved in 100mL 1:1 mixture of ethanol and water, then sodium hydroxide (3.1g, 78.8mmol) was added to it and was refluxed for half an hour. Bromoethanol was added to the above mixture at room temperature and reaction mixture was refluxed for 24 h. Ethanol was evaporated using rotavapor and extraction was done using ethyl acetate. Organic layer was dried over anhyd. Na_2SO_4 and was further purified by passing it through silica column using ethyl acetate and hexane (1:7 v/v) to get product (**4**). Yield = 7g (51 %). ^{1}H NMR (400 MHz, $CDCl_3$) δ ppm: 7.19 (dd, 1H, -CH-), 6.83 (d, 1H, -CH-), 6.75 (m, 2H, -CH- and –CH-), 4.08(m, 2H, -O-CH_2-), 3.96 (m, 2H, -CH_2-OH), 2.56 (t, 2H, -CH_2-), 2.06 (s, 1H, -OH), 1.6 (m, 2H, -CH_2-), 1.28 (m, 24H, -$(CH_2)_{12}$), 0.9 (t, 3H, -CH_3). ^{13}C NMR (100 MHz, $CDCl_3$) δ ppm: 158.67,114.87, 129.31, 121.43, 114.91, 111.52, 69.08, 61.64, 36.1, 32.01, 31.49, 29.77, 29.68, 29.61, 29.45, 29.43, 22.78, 14.22.

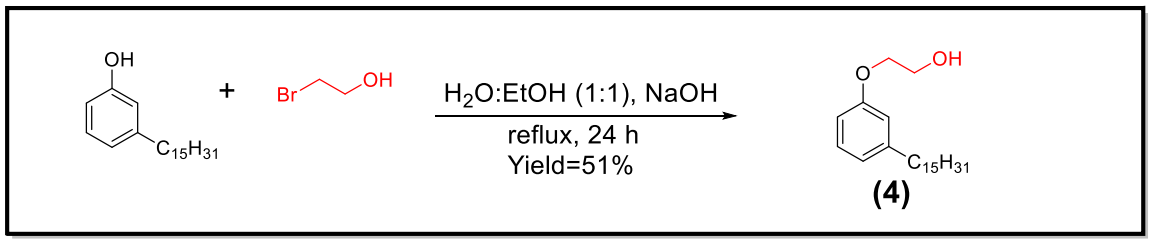

Scheme 2.4

5. Synthesis of 2-(3-pentadecylphenoxy)ethyl 3-((4-oxocyclohexyl)oxy)propanoate (**5**): compound **3** (2g, 10.75mmol) was dissolved in dry DCM (10ml) under nitrogen purging. DCC (2.9g, 13.9mmol) and DMAP (0.4g, 3.2mmol) were added into above mixture and it was stirred for 15 min at room temperature. Compound **4** dissolved in dry DCM (15ml) was added to above mixture in a dropwise manner under nitrogen purging and reaction mixture was stirred for 24 h under nitrogen. After completion of reaction DCU (byproduct) was removed out by filtration. Further purification of crude product was done by using column chromatography to get compound **5**, ethyl acetate and hexane (1:10 v/v) was used as a eluent. Yield = 3.5g (63%). ^{1}H NMR (400 MHz, $CDCl_3$) δ ppm: 7.16 (dd, 1H, -CH-), 6.79 (d, 1H, -CH-), 6.70 (m, 2H, -CH- and –CH-), 4.44(m, 2H, -(CO)-O-CH_2-), 4.17 (m, 2H, -CH_2-O-), 3.77(m, 2H, -O-CH_2), 3.7 (m,1H,-CH-O-), 2.64(t, 2H, -CH_2-(CO)-O-),2.57 (m, 4H, -CH_2-), 2.2 (m,2H, -CH2), 2.0 (m, 2H, -CH2), 1.60 (m, 2H, -CH2), 1.24 (m, 24H, -$(CH_2)_{12}$), 0.86 (t, 3H, -CH_3). ^{13}C NMR (100 MHz, $CDCl_3$) δ ppm: 211.40, 171.73, 158.51,144.89, 129.32, 121.5, 114.87, 111.47, 73.08, 65.83, 63.74, 63.16, 37.14, 36.1, 35.4, 32.01, 31.49, 30.51, 29.77, 29.68, 29.61, 29.45, 22.78, 14.21.

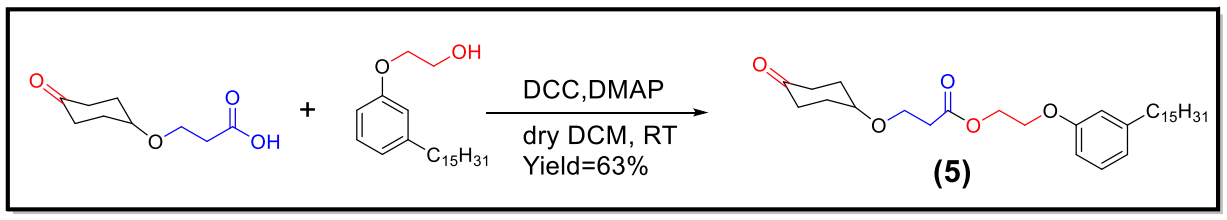

Scheme 2.5

6. Synthesis of 2-(3-pentadecylphenoxy)ethyl 3-((7-oxooxepan-4-yl)oxy)propanoate (**6**): Compound **5** (4g, 7.7mmol) was dissolved in dry DCM (120ml). sodium bicarbonate (4g, 23.2mmol) and mCPBA (1.95g, 23.2mmol) were sequentially added into above mixture and reaction mixture was stirred at room temperature for 24 h under nitrogen condition. Reaction mixture was quenched using saturated solution of $Na_2S_2O_3$ and $NaHCO_3$ and crude product was extracted in DCM. Organic layer was dried by passing it through anhyd. Na_2SO_4 and it was further purified using column chromatography to get product **6**, ethyl acetate and hexane (1:15 v/v) was used as an eluent. Yield = 3.5g (85%). ^{1}H NMR (400 MHz, $CDCl_3$) δ ppm: 7.19 (dd, 1H, -CH-), 6.79 (d, 1H, -CH-), 6.73 (m, 2H, -CH-), 4.44(m, 3H,-(CO)-O-CH_2- and -(CO)-O-CH-),4.17(m,2H,-CH_2-O-), 3.99 (m, 1H, -O-CH-) 3.72(m, 3H, -O-CH_2 and –O-CH-), 2.93 (m, 1H, -O-(CO)-CH-), 2.63(m, 2H, -CH_2-(CO)-O-), 2.57 (m, 2H, -CH_2-), 2.37 (m,1H, O-(CO)-CH-), 2.0 (m, 2H, -CH_2), 1.78 (m, 2H, -CH_2), 1.61 (m, 2H, -CH_2), 1.24 (m, 24H, -$(CH_2)_{12}$), 0.86 (t, 3H, -CH_3). ^{13}C NMR (100 MHz, $CDCl_3$) δ ppm: 176.12, 171.61, 158.48, 144.94, 129.36, 121.56, 114.82, 111.44, 65.82, 63.61, 63.23, 36.1, 35.31, 33.9, 32.01, 31.5, 29.78, 29.69, 29.45, 27.81, 27.31, 22.78, 14.22.

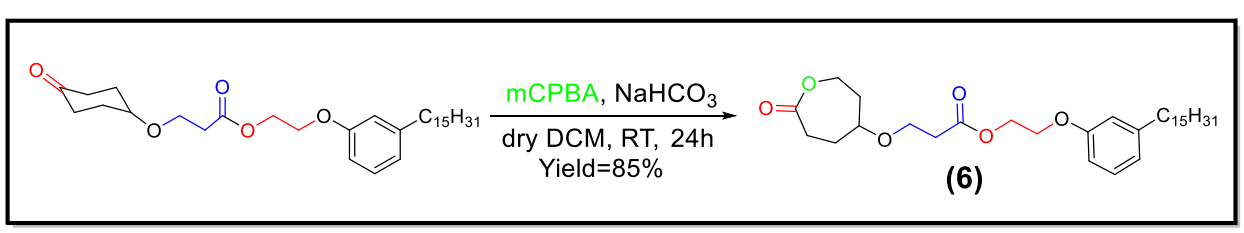

Scheme 2.6

7. Synthesis of tert-butyl 3-((7-oxooxepan-4-yl)oxy)propanoate (**7**): compound **2** (6g, 24.7mmol) was dissolved in dry DCM (180ml). sodium bicarbonate (6.25g, 74.4mmol) and mCPBA (12.81g, 74.4mmol) were sequentially added into above mixture and reaction mixture was stirred at room temperature for 24 h under nitrogen condition. Reaction mixture was quenched using saturated solution of $Na_2S_2O_3$ and $NaHCO_3$ and crude product was extracted in DCM. Organic layer was dried by passing it through anhyd. Na_2SO_4 and it was further purified using column chromatography to get product **7**, ethyl acetate and hexane (1:15 v/v) was used as an eluent. Yield = 4.8g (75%). ^{1}H NMR (400 MHz, $CDCl_3$) δ ppm: 4.46(m, 1H, -(CO)-O-CH-), 4.01 (m, 1H, -O-CH-) 3.67(m, 3H, -O-CH_2 and –O-CH-), 2.96 (m, 1H, -O-(CO)-CH-), 2.46(m, 2H, -CH_2-(CO)-O-), 2.38 (m,1H, O-(CO)-CH-), 2.0 (m, 2H, -CH_2), 1.79 (m, 2H,-CH_2-), 1.44 (m, 24H, -$C(CH_3)_3$). ^{13}C NMR (100 MHz, $CDCl_3$) δ ppm: 176.11, 170.87, 80.69, 73.93, 63.94, 63.30, 36.48, 33.87.

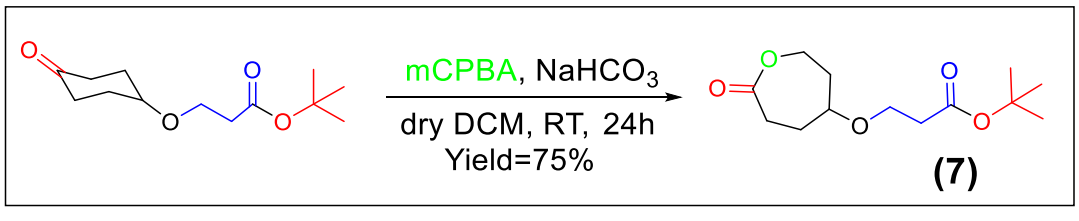

Scheme 2.7

8. Synthesis of 4-(1,2,2-triphenylvinyl)phenol **(8)**: 4-Hydoxybenzophenone (7g, 0.035mol), benzophenone (6.43g, 0.035mol) was dissolved in dry THF (105 ml) under nitrogen and Zn dust (5.77g, 0.088mol) was added to it and this mixture was refluxed for 10 min. After 10min TiCl4 was added to it at 0 ^{o}C with continuous stirring and reaction was refluxed for 24 hours. Upon completion of reaction THF was evaporated and acidic work up (1N HCL and ethyl acetate) was done to remove Zn dust. Organic layer was dried by passing it through anhyd. Na_2SO_4 and it was further purified using column chromatography to get product **8**, ethyl acetate and hexane (1:15 v/v) was used as an eluent. Yield = 3g (25%). ^{1}H NMR (400 MHz, $CDCl_3$) δ ppm: 6.57(d, 2H, -CH-), 6.90 (d, 2H,-CH-), 7.12-6.98 (m, 15H, -CH-). ^{13}C NMR (100 MHz, $CDCl_3$) δ ppm: 154.07,144.06, 143.95, 140.49, 140.26, 136.45, 132.81, 131.41, 127.78, 127.68,126.45, 126.34, 114.65

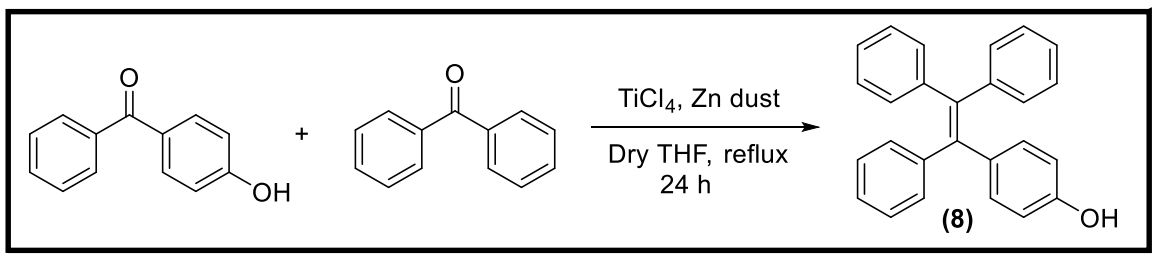

Scheme 2.8

9. Synthesis of 2-(4-(1,2,2-triphenylvinyl)phenoxy)etan-1-ol **(9)**: Compound (8) (3g, 8.61mmol) was dissolved in dry DMF (40ml) under nitrogen and K2CO3 (5.35g, 38.7mmol) was added to it and this mixture was refluxed for 45 min. chloroethoxy ethanol (1.36ml, 0.715mol) was added in a dropwise manner and then KI was added to it and reaction mixture was refluxed for 48 hours. Upon completion of reaction DMF was evaporated using rota-evaporator and work up (ice cold water and ethyl acetate) was done to remove K_2CO_3, KI and residual DMF. Organic layer was dried by passing it through anhyd. Na_2SO_4 and it was further purified using column chromatography to get product **9**, ethyl acetate and hexane (1:15 v/v) was used as an eluent. Yield = 3g (65.21%). ^{1}H NMR (400 MHz, $CDCl_3$) δ ppm: 6.67(d, 2H, -CH-), 6.93 (d, 2H,-CH-), 4.07(t, 2H, -O-CH2-), 3.84 (t, 2H, -O-CH2-), 3.76(t, 2H, -O-CH2-),

3,67 (t, 2H, HO-CH2-). ^{13}C NMR (100 MHz, $CDCl_3$) δ ppm: 157.21, 144.00, 140.50, 140.26, 136.57, 132.63, 131.42, 127.80, 127.68, 126.44, 126.34, 113.75, 72.63, 69.77, 67.23, 61.87.

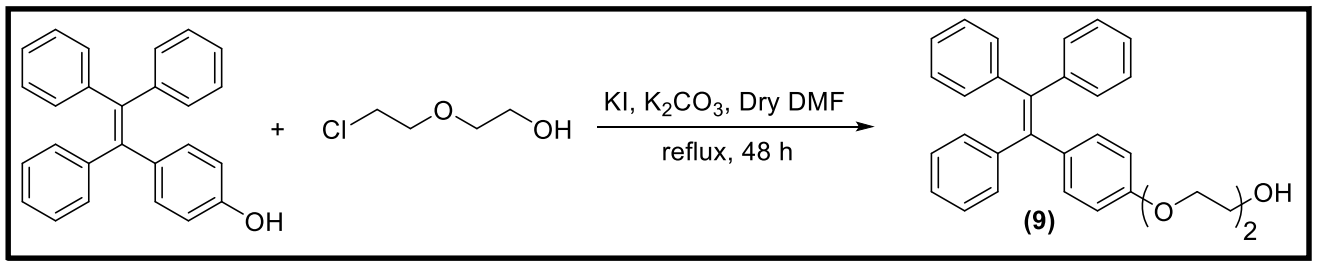

Scheme 2.9

10. Synthesis of polycaprolactone: To synthesize the polymer with 100 repeating unit, the initial monomer to initiator ratio ($[M_0]/[I_0]$) was taken to be 100. Polyethylene glycol (87.6mg, 0.044mmol) as a initiator, caprolactone (500mg, 4.38mmol) and catalyst $Sn(Oct)_2$ (8.87mg, 0.022mmol) were weighed in oven dried schlenk tube. This reaction mixture was kept on high vacuum for 45 min at room temperature and then the schlenk tube was dipped into a preheated (110 ^oC) oil bath for 4 h under constant stirring. After 4 h, polymer was dissolved in THF and was precipitated in cold methanol to get the pure polymer. Yield = 350mg (59.5%)

^{1}H NMR (400 MHz, $CDCl_3$) δ ppm: 4.05 (t, 2H), 3.63 (s, 1.88H), 3.37(s. 0.03H), 2.3 (t, 1.99H), 1.63 (m, 4H), 1.37 (m, 2H)

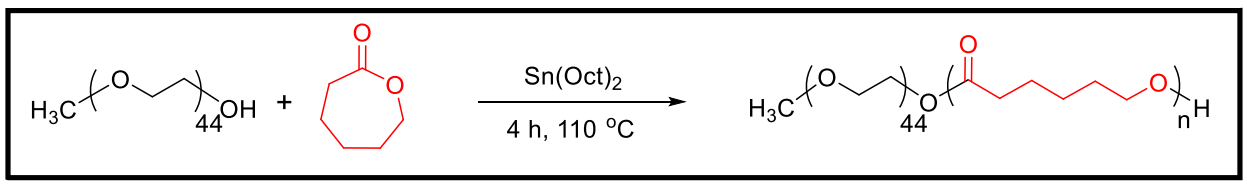

Scheme 2.10

11. Synthesis of PEG-b-PPCL: To synthesize the polymer with 50 repeating unit, the initial monomer to initiator ratio ($[M_0]/[I_0]$) was taken to be 50. Polyethylene glycol (2K) (30.03mg, 0.015mmol) as a initiator, PDP substituted caprolactone **6** (400mg, 0.75mmol) and catalyst $Sn(Oct)_2$ (3.0mg, 0.0075mmol) were weighed in oven dried schlenk tube. This reaction mixture was kept on high vacuum for 45 min at room temperature and then the schlenk tube was dipped into a preheated (130 ^oC) oil bath for 8 h under constant stirring. After 8 h, polymer was dissolved in THF and was precipitated in cold methanol to get the pure polymer. Its formation was confirmed by ^{1}H NMR (Figure 3.5) Yield = 300mg (69.7 %)

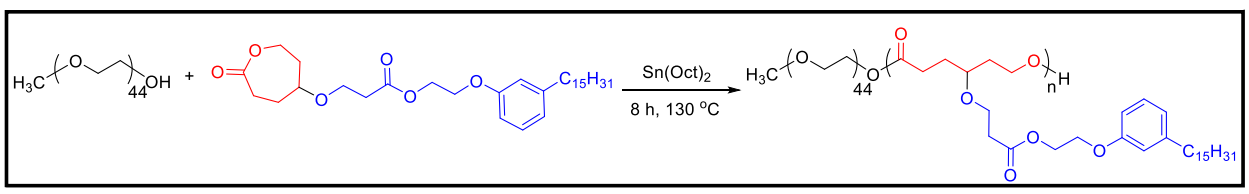

Scheme 2.11

12. Synthesis of TPE-$PPCL_{10}$: To synthesize the polymer with 10 repeating unit, the initial monomer to initiator ratio ($[M_0]/[I_0]$) was taken to be 10. TPE-OH (40.97mg, 0.09385mmol) as a initiator, PDP substituted caprolactone **6** (500mg, 0.9385mmol) and catalyst $Sn(Oct)_2$ (19.01mg, 0.0469mmol) were weighed in oven dried schlenk tube. This reaction mixture was kept on high vacuum for 45 min at room temperature and then the schlenk tube was dipped into a preheated (130 ^oC) oil bath for 8 h under constant stirring. After 8 h, polymer was dissolved in THF and was precipitated in a mixture of cold 70%

diethyl ether and 30% methanol to get the pure polymer. Its formation was confirmed by ^{1}H NMR (Figure 5.3) Yield = 320mg (61.7 %)

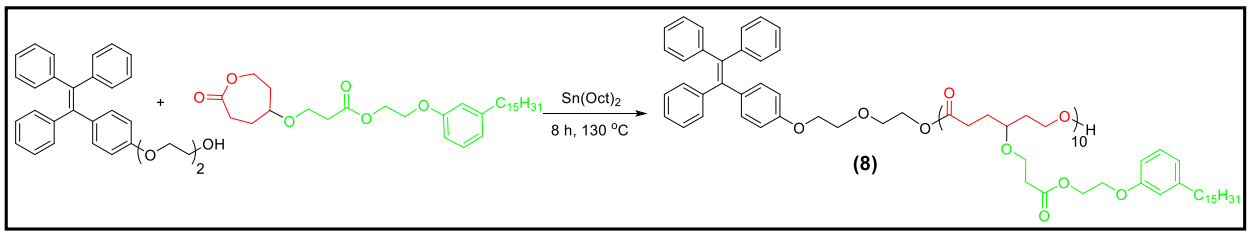

Scheme 2.12

13. Synthesis of TPE-PPCL$_{10}$-b-BPCL$_{50}$: To synthesize a block copolymer with 50 repeating unit of BPCL, the initial monomer to macro-initiator ratio ([M$_0$]/[I$_0$]) was taken to be 10. TPE-PPCL$_{10}$ (223.157mg, 0.0387mmol) was used as macro-initiator, butyl ester substituted caprolactone **7** (500mg, 1.9357mmol) and catalyst Sn(Oct)$_2$ (7.84mg, 0.0193mmol) were weighed in oven dried schlenk tube. This reaction mixture was kept on high vacuum for 45 min at room temperature and then the schlenk tube was dipped into a preheated (130 °C) oil bath for 6 h under constant stirring. After 6 h, polymer was dissolved in THF and was precipitated in a mixture of cold 50% diethyl ether and 50% methanol to get the pure polymer. Its formation was confirmed by ^{1}H NMR (Figure 5.4) Yield = 412 mg (56.9 %)

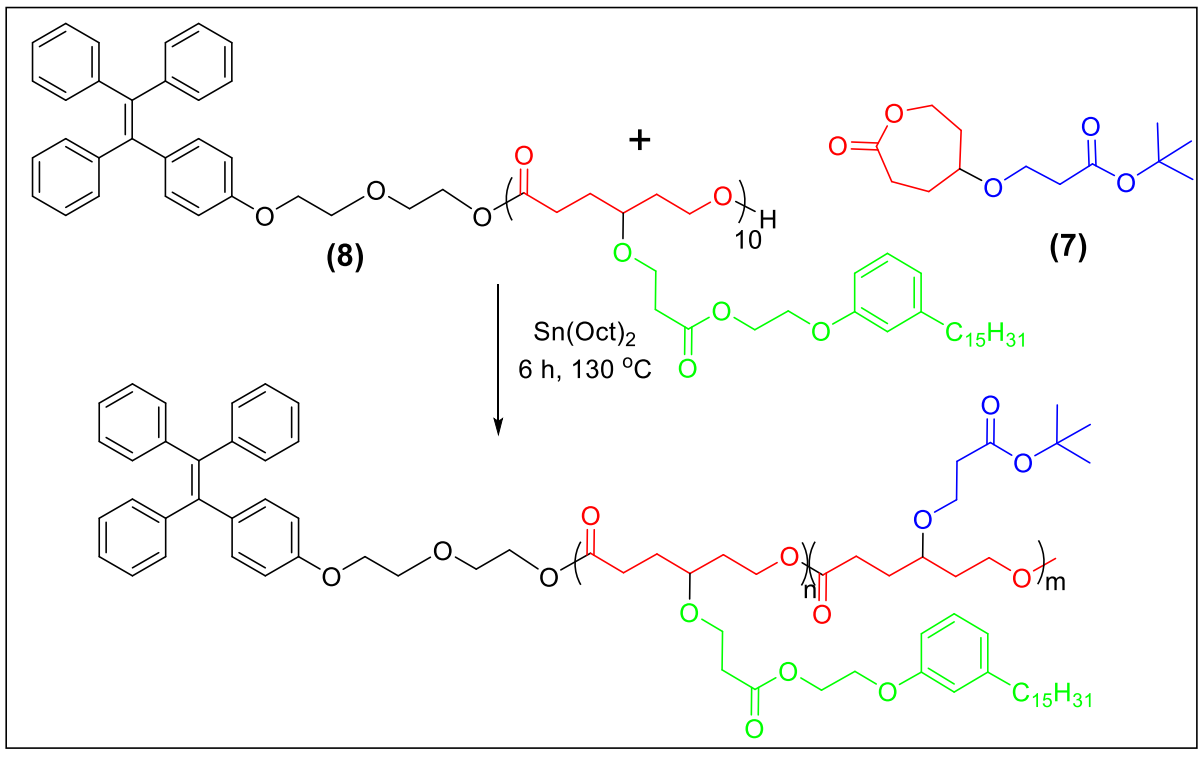

Scheme 2.13

14. Synthesis of TPE-PPCL$_{10}$-b-CPCL$_{50}$: Polymer TPE-PPCL$_{10}$-b-BPCL$_{50}$ (100mg) was taken in round bottom flask and TFA (1ml) was slowly added to it at 0 °C followed by sonication to dissolve the polymer completely. Above mixture was constantly stirred at 0 °C for 30 min for complete deprotection. Upon completion DCM was added to the reaction, and solvent (DCM+TFA) was evaporated using rota-evaporator and this was repeated three times for complete removal of TFA. Its formation was confirmed by ^{1}H NMR (Figure 5.5) Yield = 82 mg (82 %)

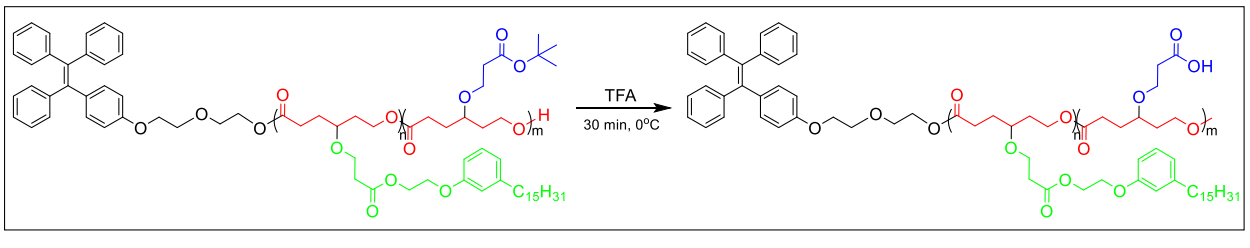

Scheme 2.14

2.4 Self Assembly of Polymers: It was done by dissolving 3mg of polymer in a 0.5 ml of DMSO and then this solution was added into 2.5 ml of water in a dropwise manner under constant stirring at room temperature, this mixture was stirred for 3 h. This 3 ml solution was then transferred into a dialysis tube (MWCO= 1000) and dialyzed against water. Water was changed at regular intervals to remove the DMSO from the tube and thus facilitate the self assembly of polymer.

2.5 Nile red encapsulation in Polymers: 3 mg of polymer and 0.1 mg of nile red was dissolved in 0.5 ml of DMSO. The above solution was then added into 2.5 ml of water in a dropwise manner under constant stirring at room temperature and the mixture was stirred for 3 h. This 3 ml solution was then transferred into a dialysis tube (MWCO= 1000) and dialyzed against water. Water was changed at regular intervals to remove the DMSO from the tube and thus facilitate the self assembly of polymer.

2.6 CMC determination using pyrene probe: various concentrations of polymer solutions starting from 1mg/ml to 10^{-7} mg/ml were made in water and transferred into vials containg pyrene probe maintained at 0.6 µM. These vials were then sonicated for 3 hours and allowed to equilibrate for 12 hours at room temperature. Vials were again sonicated for ½ an hour and let to equilibrate for 10 min before recording the fluorescence spectra to get I1/I3 plot.

2.7. Encapsulation of Doxorubicin: anticancer drug doxorubicin, commercially available as DOX.HCL (0.3 mg) was dissolved in DMSO (100 µl) and was neutralized using tri-ethyl (5 equivalents) amine and for complete neutralization, above mixture was stirred for 30 min. Polymer (3 mg) was dissolved in 400 µl of DMSO and above mixture was added into and whole mixture was stirred for 10 min. The above solution was then added into 2.5 ml of water (to get polymer concentration of 1 mg/ml) in a dropwise manner under constant stirring at room temperature and the mixture was stirred for 3 h. This 3 ml solution was then transferred into a dialysis tube (MWCO= 1000) and dialyzed against water. Water was changed at regular intervals to remove the un-encapsulated DOX and DMSO from the tube and thus facilitate the self assembly of polymer. DLC (Drug loading content) and DLE of the self assemblies were calculated using following equations:

$$DLC = \left(\frac{Weight\ of\ encapsulated\ DOX}{Weight\ of\ polymer}\right) \times 100\ \%$$

$$DLE = \left(\frac{Weight\ of\ encapsulated\ DOX}{Weight\ of\ DOX\ in\ the\ feed}\right) \times 100\ \%$$

2.8 Degradation studies of Polymer in PBS buffer by DLS method: to study the degradation of polymer in the presence and absence of esterase enzyme, change in the size of nano-assemblies was monitored using DLS. Dialyzed polymer solution (0.6 ml) was mixed with 1.2 ml of PBS and stirred at 37 °C, DLS readings were taken after every 1 hour by taking 1ml of the above solution, which was transferred back again. Same procedure was followed to study the effect of esterase, by dissolving 2 mg of esterase in the solution (as described above).

2.9 Cell Viability assay (MTT Assay): to check the cytotoxic effect of the nascent polymer, MTT assay was performed in MCF 7 cancer line using tetrazolium salt, 3-(4,5-dimethylthiazol-2-yl)-2,5-diphenyltetrazolium bromide (MTT). In each well of 96 well plate 10^3 cells were seeded using 100 µL of DMEM with 10% FBS

(fetal bovine serum) and this setup was left undisturbed for 16 h for cells to adhere. Upon completion, media was removed and varied concentration of DOX loaded polymer assemblies were added into each well, control used for all these experiments was DMEM with FBS alone. Incubation of cells was done for 72 h without changing the media, and further the media was aspirated. Further cells were treated with MTT (100 µl, 0.5 mg/ml) and after 4 h at 37 °C. After incubation the media was aspirated and formazan crystals (purple), which formed due to action of mitochondrial dehydrogenase enzyme on MTT were dissolved in DMSO (100 µl) and absorbance was taken. The microplate reader at 570 nm (Variaskan Flash) was used to record the absorbance of all the samples.

2.10 Confocal microscopy to study cellular uptake of doxorubicin loaded nano-assemblies: Cells (MCF 7) at a density of 10^5 were seeded onto coverslips, which were placed in 6-well plates containing DMEM media with 10% FBS and whole setup was incubated at 37 °C for 16 h. Cells were treated with DOX loaded nano-scaffolds and DOX at 37 °C for 4 h in a CO_2 incubator. Aspiration of drug containg media was done and cells were washed twice with PBS (1 ml) and fixed with paraformaldehyde solution (4%) in PBS at 4 °C for 15 min. Cells were again washed twice with 1 ml PBS, this was followed by staining of cells with DAPI solution in PBS and incubation at room temperature for 2 min in dark. Excess of dye was removed from the plate by PBS washing and cells were rinsed for 1min using PBS. Coverslips were mounted onto the slides using 70% glycerol medium and then dried overnight in the dark at room temperature. Images were recorded using LSM 710 Confocal microscope. ImageJ software was used to analyze these images.

3. Results and Discussion:

3.1 Synthesis and characterization of monomer:

A new PDP substituted caprolactone monomer was synthesized by multistep synthesis as shown in the **scheme 3.1**. Mono substituted product **1** was obtained by Michael addition of tert-butyl acrylate to cyclohexanediol, product **1** was further oxidized to ketone to get **2** by using PCC as an oxidizing agent and this was further deprotected to carboxyl acid derivative **3** using TFA. For coupling of PDP with the acid, PDP was first coupled with bromoethanol by SN_2 mechanism to get **4,** which was then coupled with **3** by using DCC as a coupling reagent to get **5.** Finally PDP substituted caprolactone monomer **6** was obtained by Baeyer villager oxidation of **5**. ^1H NMR spectra were used to analyze all the intermediate products.

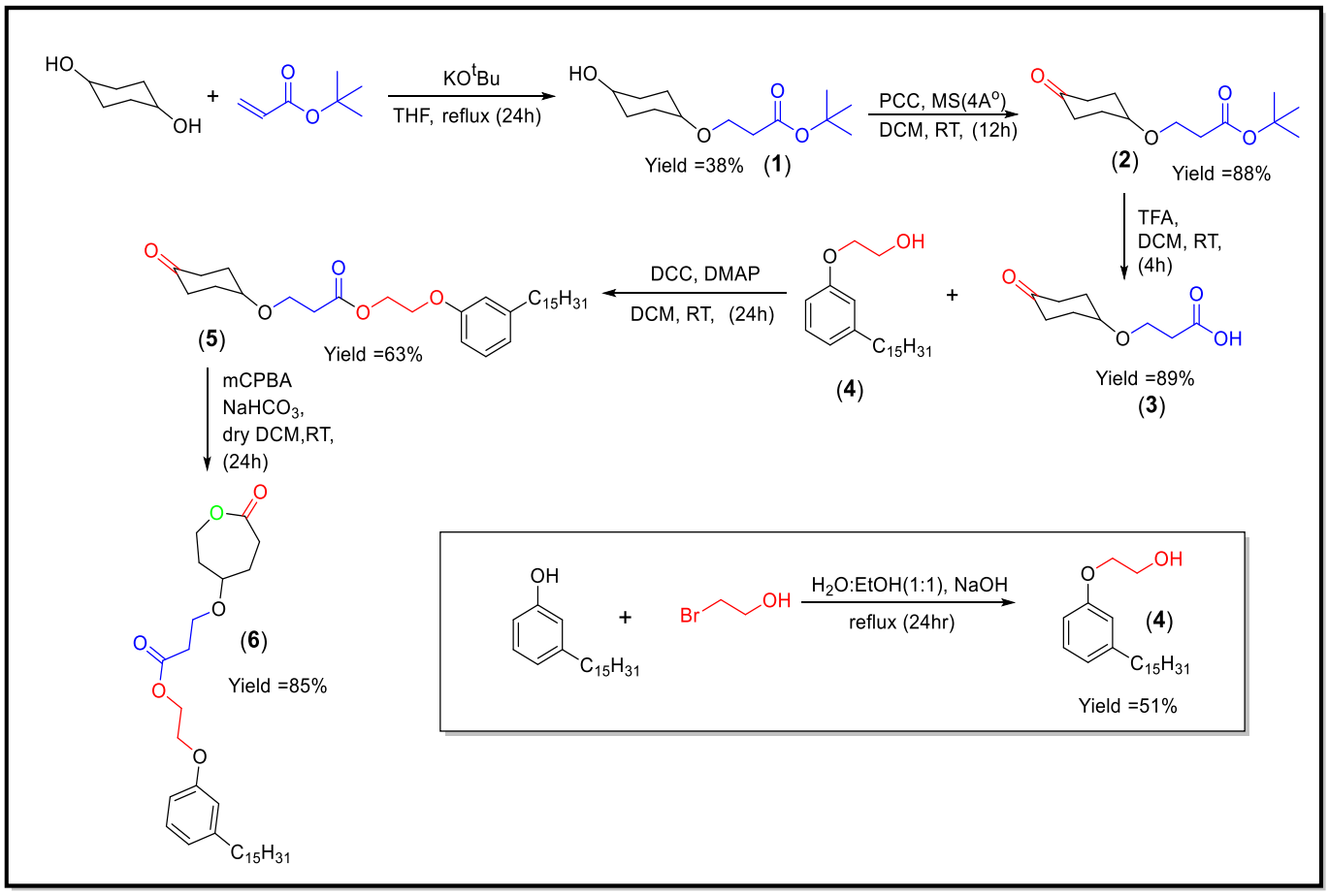

Scheme 3.1: synthesis Scheme for PDP Substituted caprolactone monomer

Figure 3.1 Shows the ^1H NMR spectra for compound 1, 2 and 3. Proton b of compound **1** shows two peaks at 3.36-3.30 ppm due to presence of cis and trans isomers of compound **1**, disappearance of peak b and downfield shift of proton D signifies the formation of ketone bond and thus confirms the formation of compound **2.**

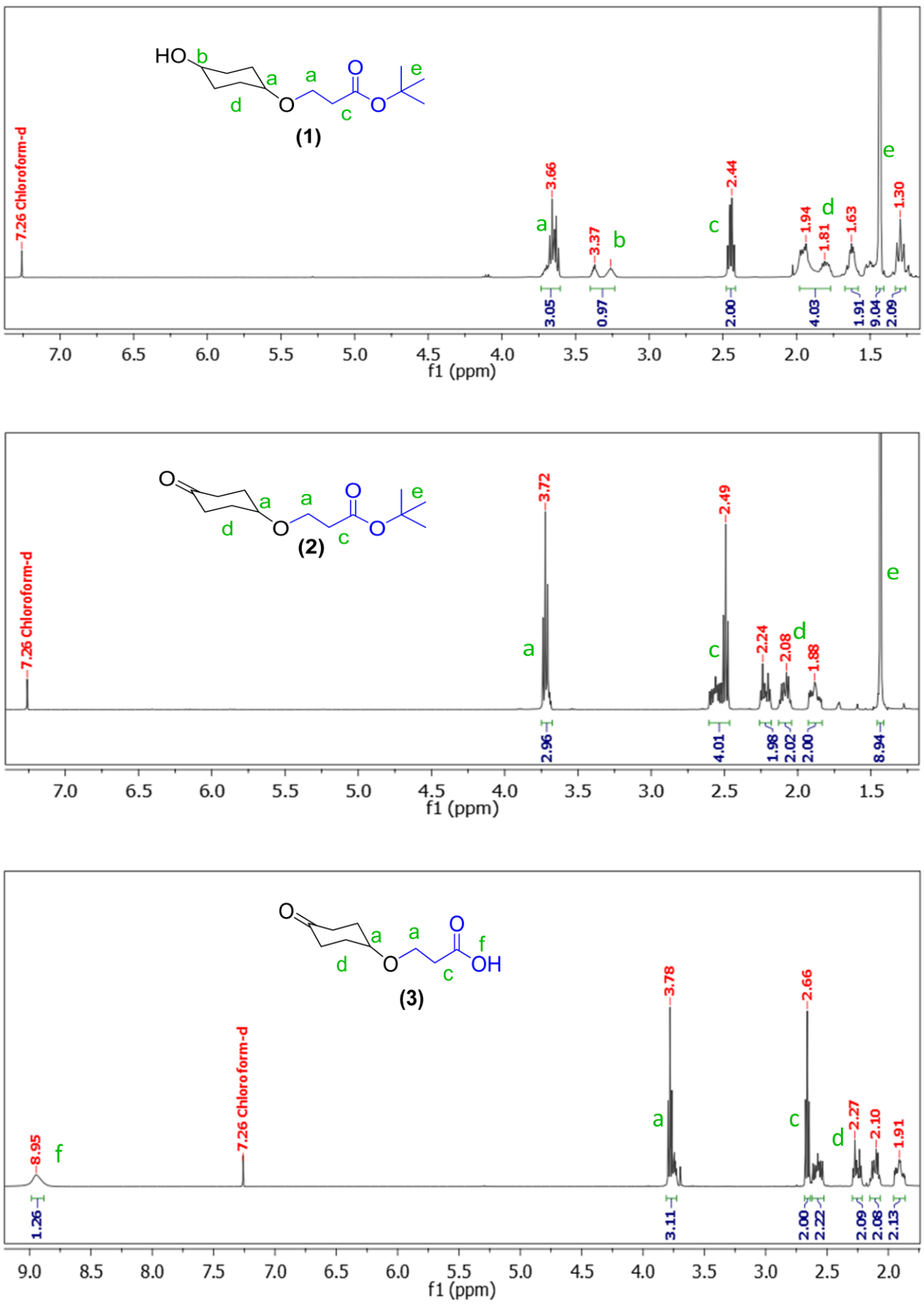

Figure 3.1: ^{1}H NMR spectra for compound 1, 2 and 3

Further formation of compound 3 is confirmed by absence of peak e in the spectra, downfield shift of proton ‘c’ due to acid formation and also the appearance of peak (f) at 8.95 ppm due to formation of acid.

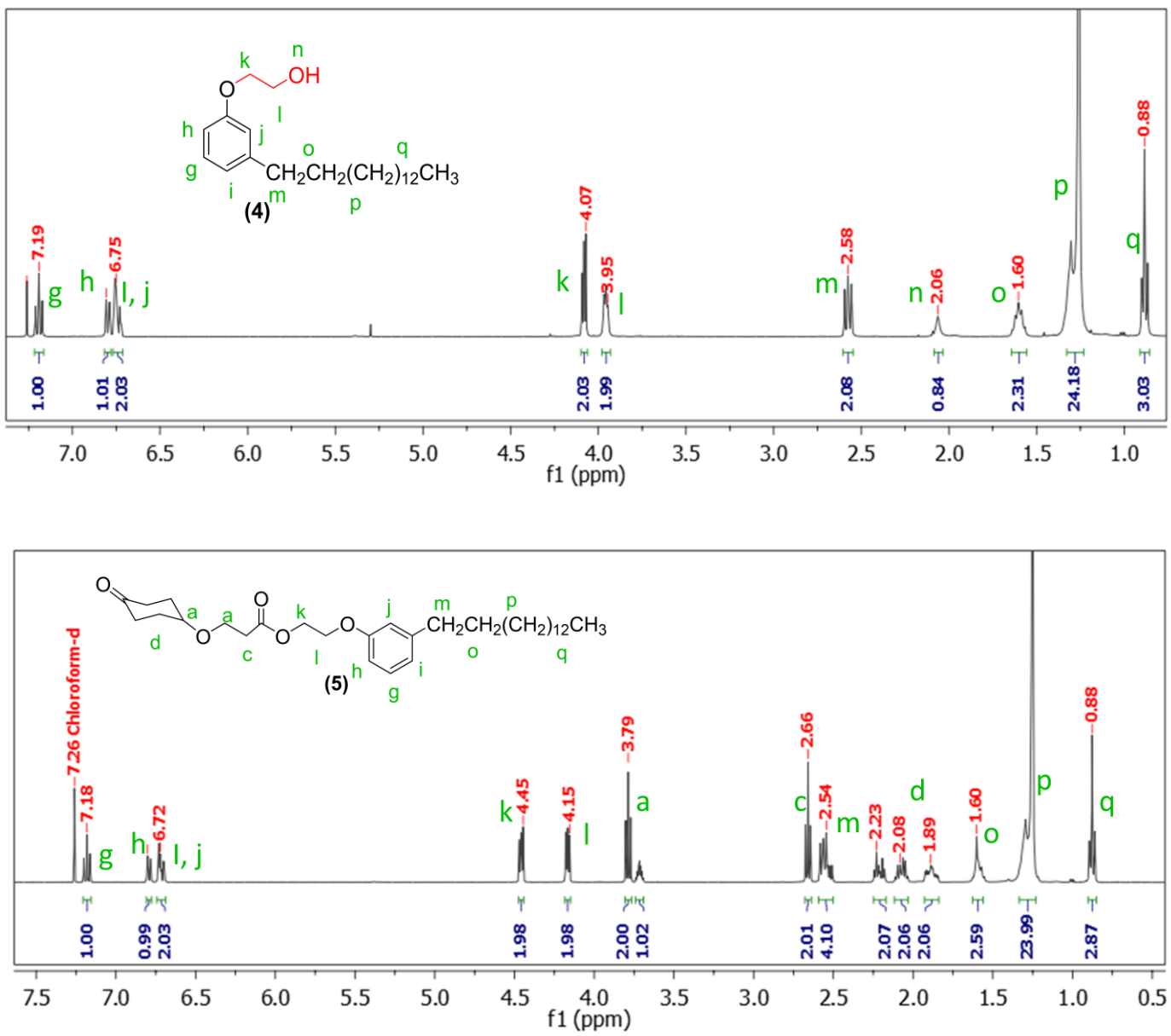

Figure 3.2: ^{1}H NMR spectra for compound 4 and 5

Formation of compound 4 is confirmed by ^{1}H NMR spectra shown in figure 3.2 and further its coupling with acid to get compound (5) is confirmed by shifting of peak '**l'** of compound **4** at 4.44 ppm (denoted as 'k' in spectra of compound 5) due to ester formation (Figure 3.2).

Formation of substituted caprolactone is confirmed by appearance of 4 new d peaks (pink and blue) at 4.45, 3.99, 2.93 and 2.38 ppm (Figure 3.3)

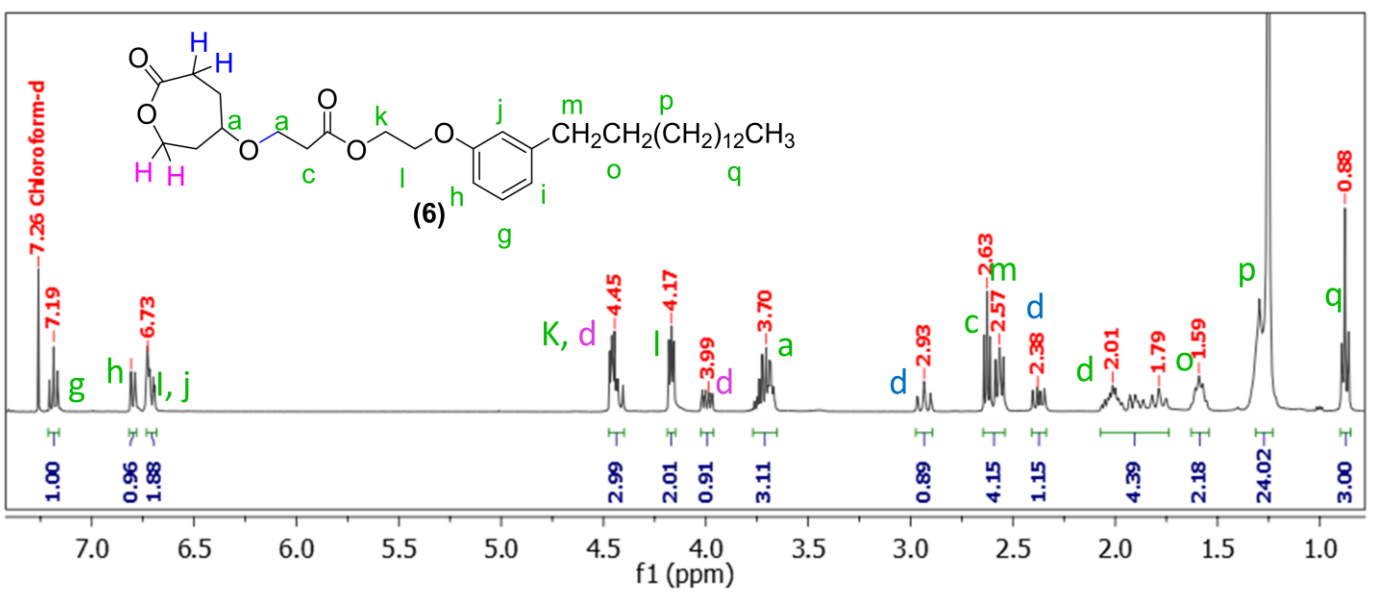

Figure 3.3: ^{1}H NMR spectra for PDP substituted caprolactone monomer

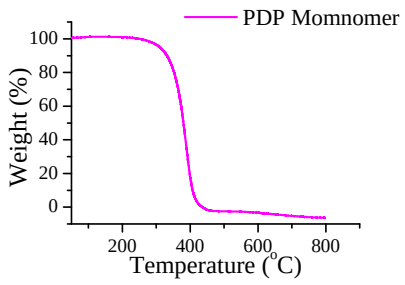

Figure 3.4: TGA for PDP monomer

Thermal stability of the monomer was determined by using TGA, and it was found that it is thermally stable upto 280 °C, thermogram of the same is shown in **figure 3.4**. It is necessary to know the thermal stability of the monomer before it underwent ROP via melt route, to make sure that it does not degrade at the polymerization temperature conditions.

3.2 Synthesis and Characterization of polymer:

PDP substituted caprolactone monomer was further ring opened at 130 °C using PEG-2K as an initiator which also acts as a hydrophilic block of the block copolymer. Tin (II) octoate was used as a catalyst, which catalyze the ROP via coordination insertion mechanism (scheme 3.2).

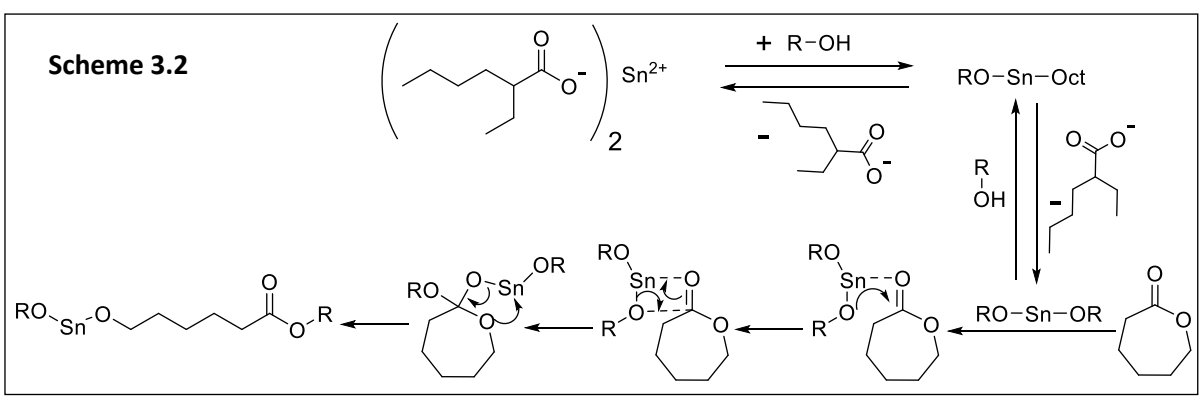

Formation of polymer was confirmed by disappearance of four ‘d’ peaks and appearance of peak ‘c’ in ^{1}H NMR spectra shown in **figure 3.5** and degree of polymerization (Xn) was obtained by comparing 3H of methyl group (b) of initiator and proton at 3.44 ppm that is ‘c’ proton from PPCL block. Proton ‘c’ gives integration of 50H on giving integration of 3 to proton ‘b’, for the feed ratio (M/I = 50) of 50.

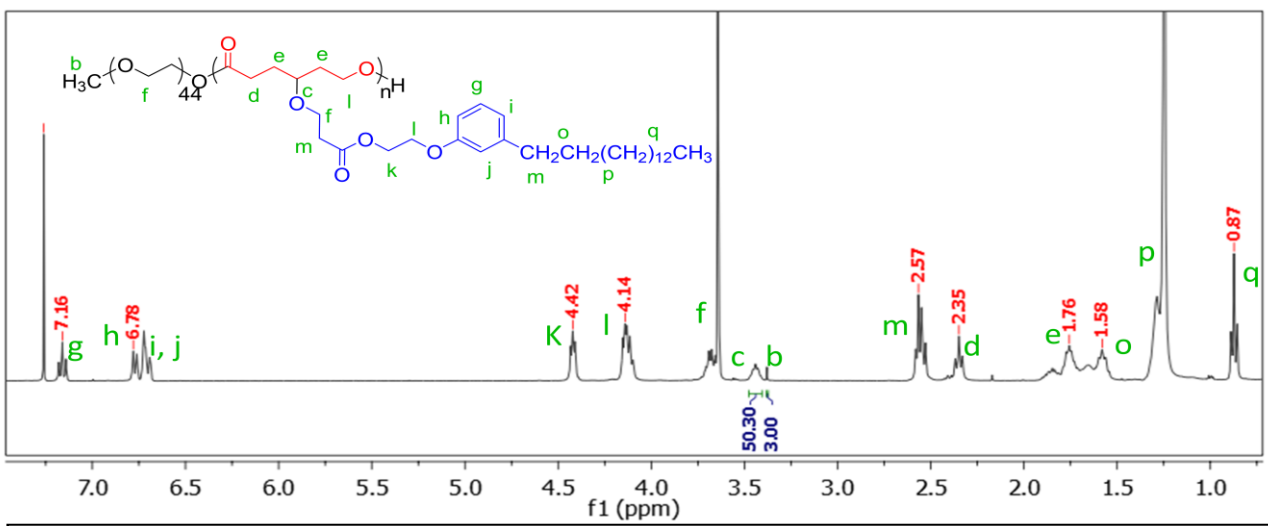

Figure 3.5: ^{1}H NMR spectra for BLOCK COPOLYMER of PEG-b-$PPCL_{50U}$

Keeping PEG-2K as a hydrophilic block, polymers with 100, 75, 25, 10 and 5 (PEG-b-$PPCL_{n=100,\ 75,\ 25,10,5}$) repeating units were also synthesized, being a controlled living polymerization technique ROP enable us to obtain polymers with desired number of repeating unit. Polymers with varied size of hydrophobic block were synthesized to optimize, the number of unit required for self assembly.

3.3 GPC, DSC and TGA Characterization of polymers:

Purity and molecular weight (Mw) of all the polymers was reconfirmed by Gel Permeation Chromatography (GPC, Figure 6), monomodal distribution of all the polymers led us to conclude that all the polymers are pure. Mw, Mn and polydispersity index (given in table 1) was also determined from GPC. When we pass the polymer dissolved in a good solvent through the GPC column, GPC or size exclusion chromatography segregate the molecules on the basis of their Mw or size, molecules with higher Mw are eluted first and then with lower Mw. It correlates the samples elution time with calibration plot, obtained from the polymer standards with known molecular weights and give us the molecular weight of unknown sample. Various calibration standards (CS) such as polyethylene oxide, dextran, polystyrene are available, depending upon the CS used, the weight of our polymer may get under or over estimated. Here we used polystyrene as a CS and THF as an eluent, from table 1 data we can see that the Mw has been underestimated this may happen because the solvation sphere of THF around the standard and our sample might be different.

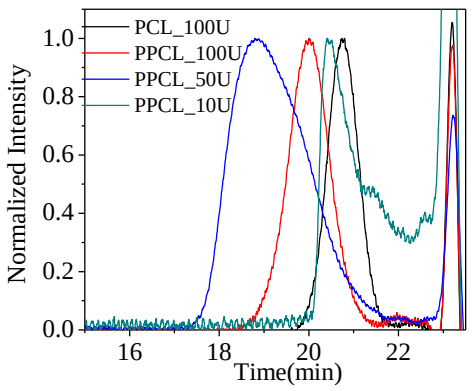

Figure 3.6: GPC chromatograms for PEG-b- PPCL$_n$

		NMR			GPC		
S. No.	Polymer	Feed (M/I)	Incorporated	Mn (g/mol)	Mn (g/mol)	Mw (g/mol)	PDI
1	PEG-b-PCL$_{100}$	100	100	13400	2800	3600	1.2
2	PEG-b-PPCL$_{10}$	10	9	6500	1600	3000	1.8
3	PEG-b-PPCL$_{50}$	50	50	28000	9000	22900	2.4
4	PEG-b-PPCL$_{100}$	100	98	54000	6700	9000	1.4

Table 3.1: ^{1}H NMR and GPC Characterization table for polymers

Thermal properties of polymer can be studied by two techniques, Differential Scanning Calorimetry (DSC) and Thermogravimetric Analysis (TGA). DSC works on the principle of a heat flow required to maintain the both the DSC pans at the same temperature, more or less heat needs to be flown to the sample pan to keep both the pans at same temperature once the sample undergoes phase transition. Upon crystallization polymer releases the heat and less heat flows to the sample pan than the reference pan and this difference can be plotted against temperature as shown in the thermograms. We can see in figure 3.7 (b) that, all the polymers are semicrystalline in nature and crystallization temperature lies between 15-25 °C, which is lesser than that of block copolymer of PEG and PCL, thus it was observed that PEG-PCL polymers are semicrystalline at room temperature but PEG-*b*-PPCL are not.

Thermal stability was determined by TGA (Figure 3.7 (a)) and it was observed that polymers are stable up to 250 °C. Thus we can say conclude that, regardless of the number of hydrophobic repeating units present in the polymer, they are highly stable up to 250 °C.

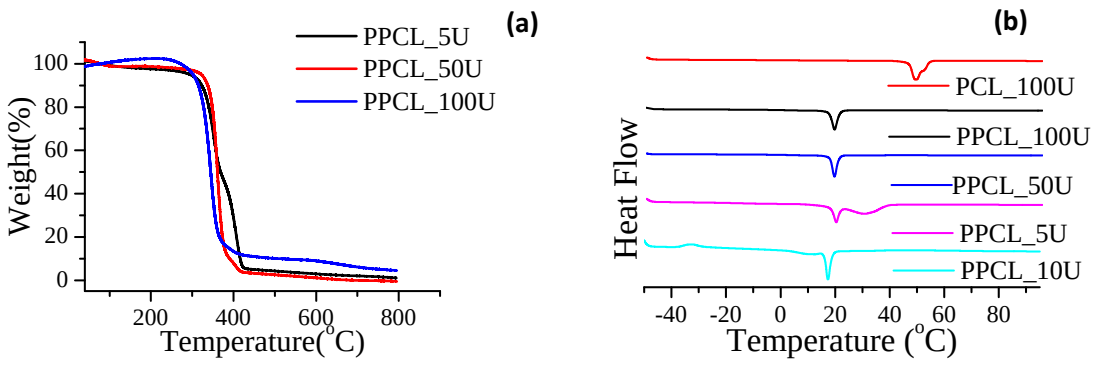

Figure 3.7: (a) TGA thermograms for polymers (b) DSC thermograms for PEG-b- PPCL$_n$

3.4 Self assembly of polymer and Nile red encapsulation:

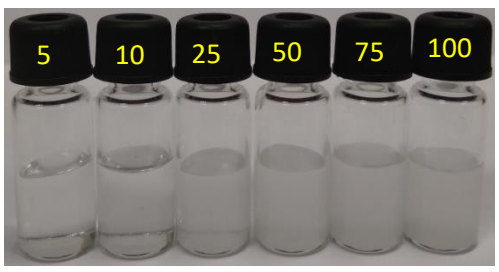

Self assembly studies (as explain in the methods) were performed tosee whether these newly synthesized polymers are forming some nanostructures. Upon dialysis of polymeric samples against water it was observed that all the polymers were dispersible in water, but some amount of precipitation was also seen in polymers with 50 and 100 repeating units. In the given image we can see that dialysed solutions of 5 and 10 repeating units are clear but that of 25, 50, 75 and 100 units are not, which tells that later polymers are highly hydrophobic in nature and thus could not form nano-assemblies. From DLS measurements (Figure 3.8 (a)), size of nanoassmblies of nascent polymer was found out to be 113 nm and 68 nm for PEG-b-PPCL$_{n=5}$ and PEG-b-PPCL$_{n=10}$ respectively.

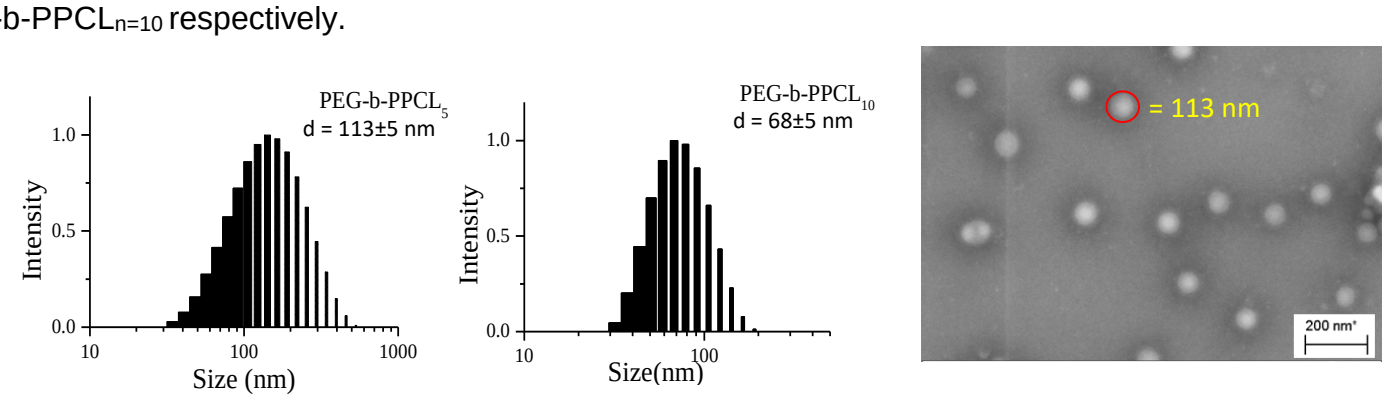

Figure 3.8: (a) DLS histogram for self assemblies of PEG-b- PPCL$_{5, 10}$ (b) FESEM for PEG-b-PPCL$_5$

As discussed in the introduction we anticipated that these block copolymers might form vesicular assemblies due to presence of PDP group for interdegitization and thus leading to bilayer formation (Figure 3.9), and to validate this idea we checked the loading of nile red (hydrophobic dye) and Rhodamine-B (being a hydrophilic dye so it can only be encapsulated in hydrophilic cavity of vesicle but not in a micelle; hence loading of Rhodamine leads one to conclude whether vesicular assemblies are formed). It was observed that PEG-b-PPCL$_{n=5,\ 10}$ could able to load nile red but not Rhodamine-B (figure 3.10 (a))and thus we can conclude that although vesicular directing group PDP is present in PEG-b-PPCL$_{n=5\ ,10}$ they are not able to form vesicles but micelles. So these polymers does not self assemble the way, we have proposed.

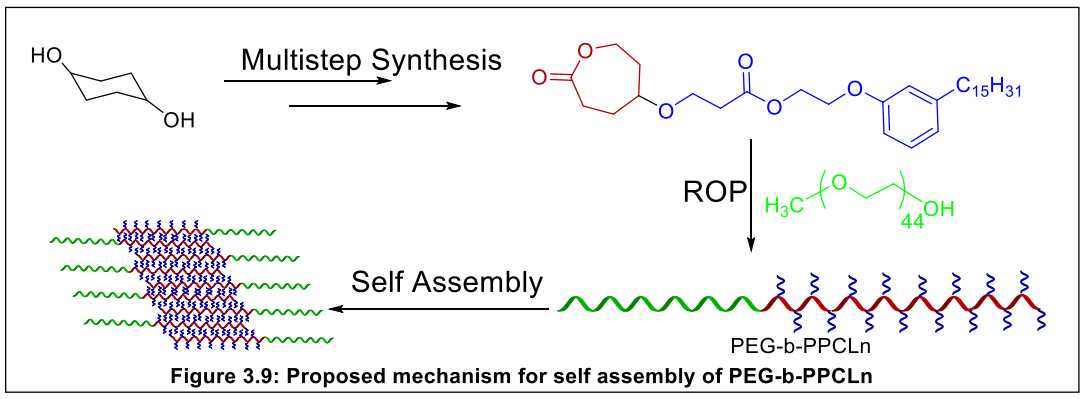

Figure 3.9: Proposed mechanism for self assembly of PEG-b-PPCLn

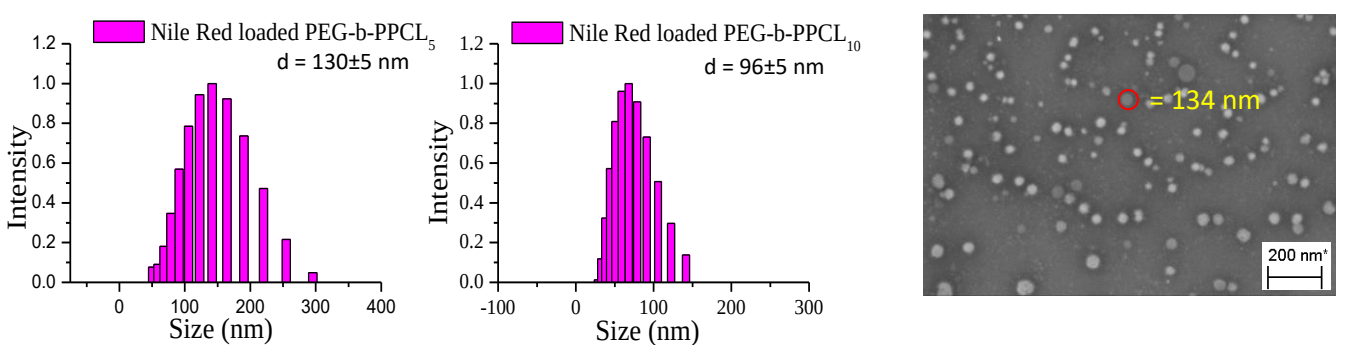

Figure 3.10: (a) DLS histogram for Nile red loaded self assemblies (b) FESEM for Nile red loaded PEG-b-PPCL$_{10}$

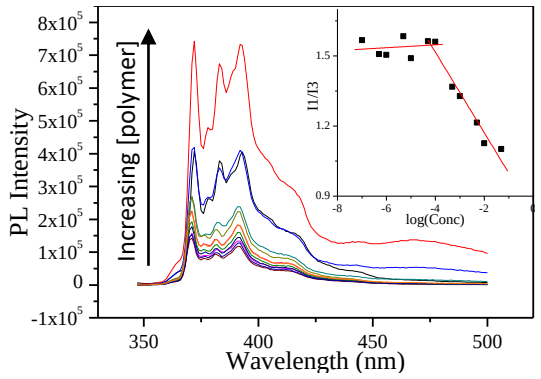

Figure 3.11: CMC determination for PEG-b-PPCL$_5$

Critical Micellar Concentration was determined by using pyrene as probe. It is known that peak I1 (372 nm) and I3 (384 nm) of pyrene fluorescence spectra are sensitive to the external environment, which it is encapsulated into. The ratio I1/I3 remains constant upto some concentration of the polymer solution and it decrease at certain concentration and then keep on decreasing and this breaking point is known as the CMC of the polymer. Here we determined the CMC by keeping the concentration 0.6 µM constant throughout and varying the polymer concentration In the inset we can see that I1/I3 plot against log of polymer concentration, the ratio remains constant till the concentration of 10^{-4} and it decreases from that point onwards, thus we can see that CMC for polymer with 5U is 10^{-4} mg/ml (Figure 3.11). similarly CMC for PEG-b-PPCL$_{10}$ was also found out to be the same.

Water contact angles were determined to check the hydrophobicity of the polymers. Polymer films were made by using polymer solution of 50 mg/ml in THF, on glass cover slips. Drop of water was placed onto the film and images were taken and water contact angle was determined for each polymer. Image and respective WCA is shown in the table 3.2 below. Hydrophilicity will be more if the WCA is smaller, we can see that polymer PEG-b-PPCL$_{10}$ is hydrophilic with WCA of 64.7º whereas all other polymers are highly hydrophobic.

Polymer	PEG-*b*-PPCL$_5$	PEG-*b*-PPCL$_{10}$	PEG-*b*-PPCL$_{25}$	PEG-*b*-PPCL$_{50}$
Image	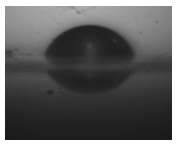	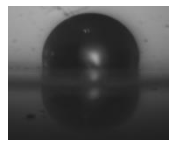	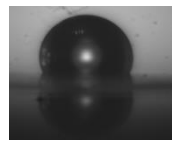	
WCA (º)	64.7	107.6	116.4	111.1

Table 3.2: Water drop images and WCA for PEG-b-PPCL

3.5 Encapsulation of Doxorubicin in the polymers:

From self assembly studies and WCA we concluded that polymers PEG-*b*-PPCL$_{25,50,75,100}$ are highly hydrophobic and are not able to self assemble and thus DOX encapsulation was studied only in PEG-*b*-PPCL$_{5,10}$. UV visible spectroscopy was used to determine the DLC and DLE (table 3.3), we can see that DLC is similar for both the polymers. To make it certain that polymeric assemblies are stable upon encapsulation was done, DLS measurements were performed and it was observed that it gives a bi-modal size distribution, which may occur because of individual and aggregated micelle formation.

UV Spectrogram of DOX loaded nano-assemblies	Polymer	PEG-*b*-PPCL$_5$	PEG-*b*-PPCL$_{10}$
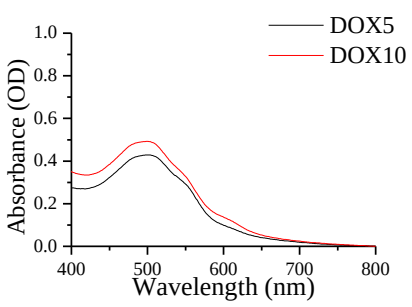	DLC (%)	2.03	2.36
	DLE (%)	20.3	23.6
	SIZE (d, nm)	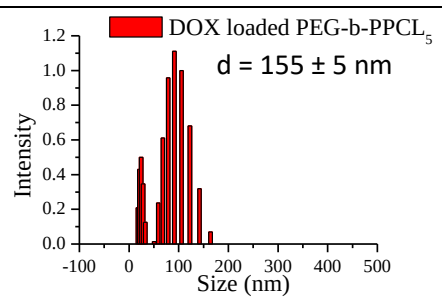	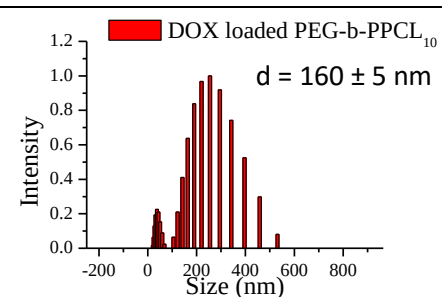

Table 3.3: UV-Visible spectra and DLS histograms for DOX loaded nano-scaffolds

3.6 Degradation studies of polymer nano-assembly:

Once the drug is encapsulated in the micelle core, the next task is to deliver and release it to the targeted site and this is possible if the polymers are biodegradable. In the backbone of PCL ester bonds are present, which can be cleaved by lysosomal or cellular enzymes such as esterase, lipases etc and to check if the polymer synthesized are biodegradable or not, in vitro degradation studies were performed in presence and absence (control) of esterase in PBS buffer (discussed in the methods). In the plot (Size Vs Time) we can see that as the time for which the polymer solution is exposed to esterase increases the size also increase, which suggests that polymeric assemblies are getting disassembled due to cleavage of ester bond present in the backbone and side groups (PDP is substituted onto PCL by ester bond), whereas size is almost stable in absence of esterase. Thus we can say that the polymers are indeed degradable in the presence of esterase and nano assemblies will be able to release the drug.

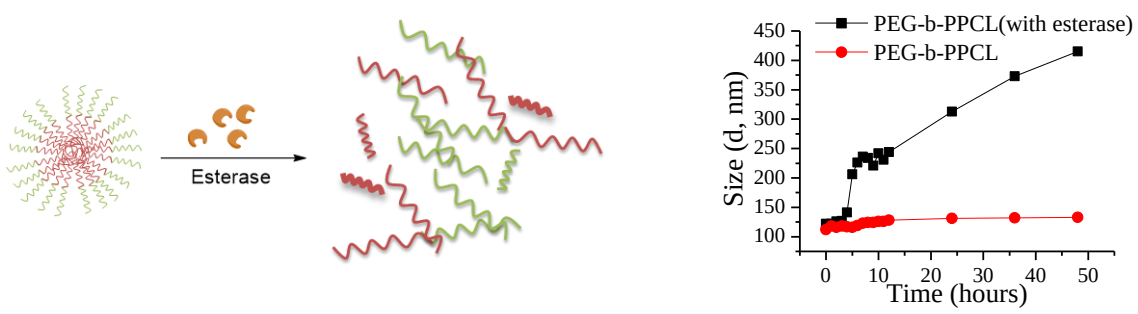

Figure 3.12: Degradation studies of polymer by DLS method

3.7 Cytotoxicity of drug loaded self assemblies:

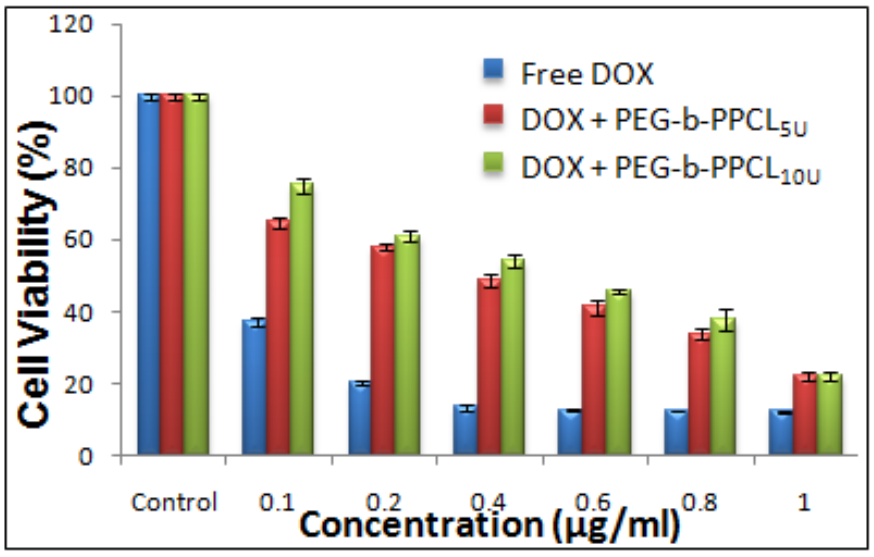

Cell viability of MCF 7 cells in presence of free DOX and DOX (drug) loaded PEG-*b*-PPCL$_{5,10}$ polymeric nano-carriers was checked using MTT assay. The DOX-loaded nano-assemblies exhibited an IC_{50} of 0.4 µg/mL, coherent with the literature values. They exhibited cytotoxicity comparable to that of the free drug. As the concentration of drug is increasing the viability of cells is decreasing or we can say that cytotoxicity is increasing.

3.8 Uptake of nanocarriers by MCF 7 cells: Cellular uptake of DOX loaded nano-scaffolds by MCF 7 cells and diffusion of free DOX in the cells was analyzed by using confocal laser scanning microscopy (CLSM). DAPI stain was used to stain nucleus. red (λ=561 nm) and blue (λ=405 nm) channels (shown in figure 3.13) were used to visualize DOX and DAPI stained nucleus respectively. We can see in the first panel (free DOX) that, DOX is mostly accumulated in the nucleus due to free diffusion whereas in case of DOX loaded polymer nanocarriers, they are mostly found in the perinuclear region and negligibly at the nucleus, moreover uptake of these nanocarriers is also very less. Scale bar for all the images is 10 μm (not properly visible in the image below).

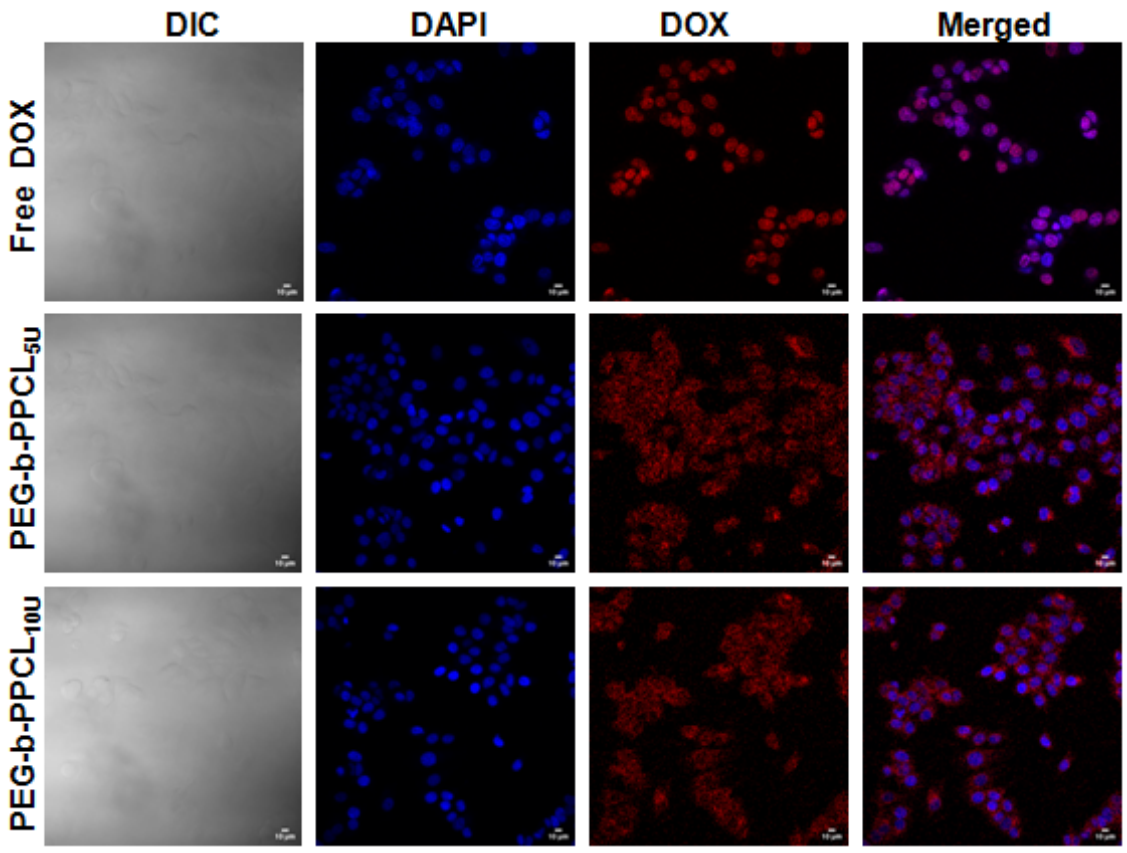

Figure 3.13: cellular uptake studies by Confocal microscopy imaging

Conclusion:

PDP substituted caprolactone monomer was successfully synthesized by multistep synthesis. Amphiphillic diblock copolymers were obtained by ring opening of this monomer to get polymers with narrow PDI. From self assembly, nile red encapsulation and DOX loading of these polymers we can conclude that only polymers with optimized hydrophobic block length (PEG-b-PPCL$_{n=5,10}$) can self assemble into nanostructures and shows nile red and DOX loading. Inability of these polymers to form vesicular assembly, led us to the conclusion that, not only PDP incorporation helps in vesicular assembly, but also the combination of other factors such as optimized hydrophobic and hydrophilic balance is required for getting vesicular assemblies.

To make this system more versatile we thought of adding functional polymeric block (CPCL, discussed in introduction) and fluorescent molecule, TPE, which makes the polymer fluorescent and enables us to know the fate of polymer upon encapsulation of drug or cellular uptake.

5. Fluorescent block-copolymers:

Once the hydrophobic block for above polymers was optimized for self assembly of above amphiphillic block copolymer (PEG-b-PPCLn), we tried to incorporate fluorescent molecule TPE (2-(4-(1,2,2-triphenylvinyl)phenoxy)etan-1-ol **(9),** which shows emission only upon aggregation and this property might help us to use nanoassmblies of these polymers for bio-imaging purpose) as an initiator and CPCL as a functional hydrophilic block and studied its effect onto the self assembly.

5.1. Synthesis and characterization of BPCL monomer and initiator:

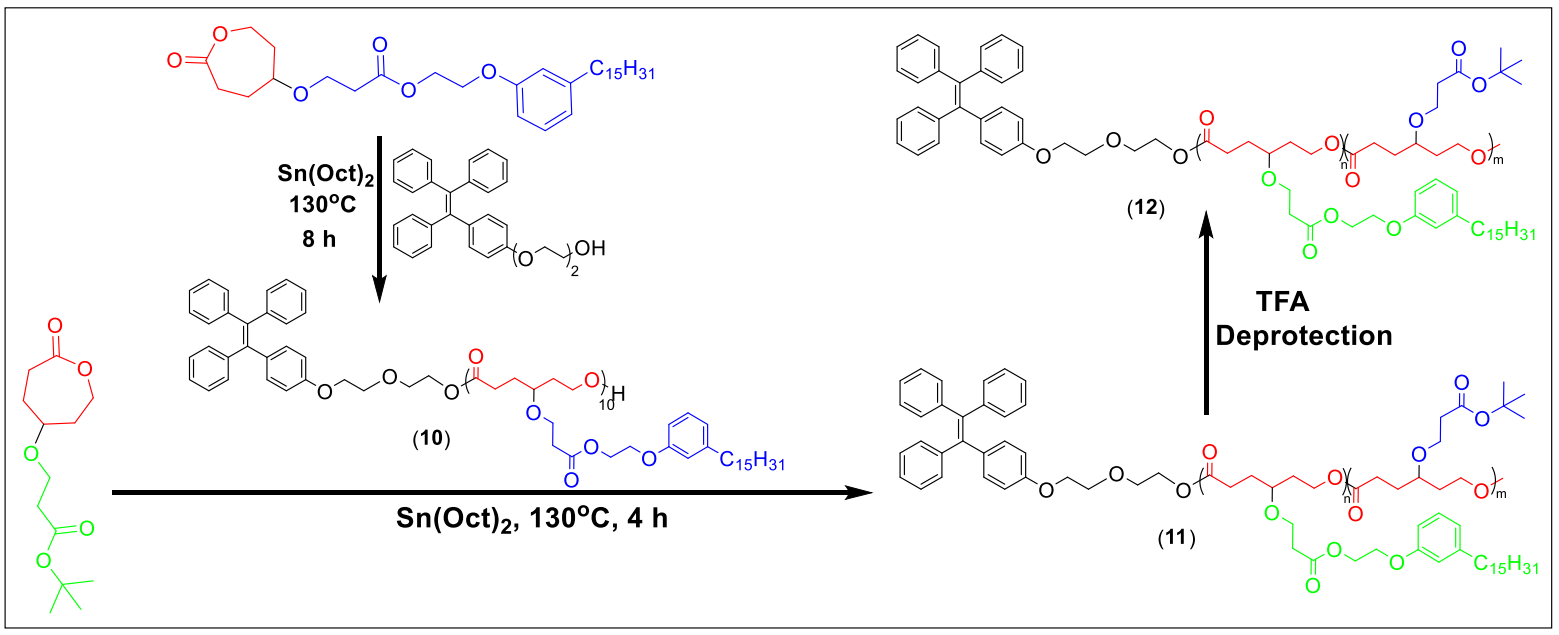

Scheme 5.1: Synthesis scheme for polymer, TPE-PPCL$_n$- CPCL$_m$

McMurry coupling of benzophenone and 4-hydroxybenzophenone (explained in experimental section) was done to obtain Compound (**8**), formation of this in confirmed by 1H NMR spectra shown in the figure, compound (**8**) was further coupled with Chloroethoxy ethanol to get compound (**9**), appearance of 4 peaks that is, u,v,w and x confirms its formation.

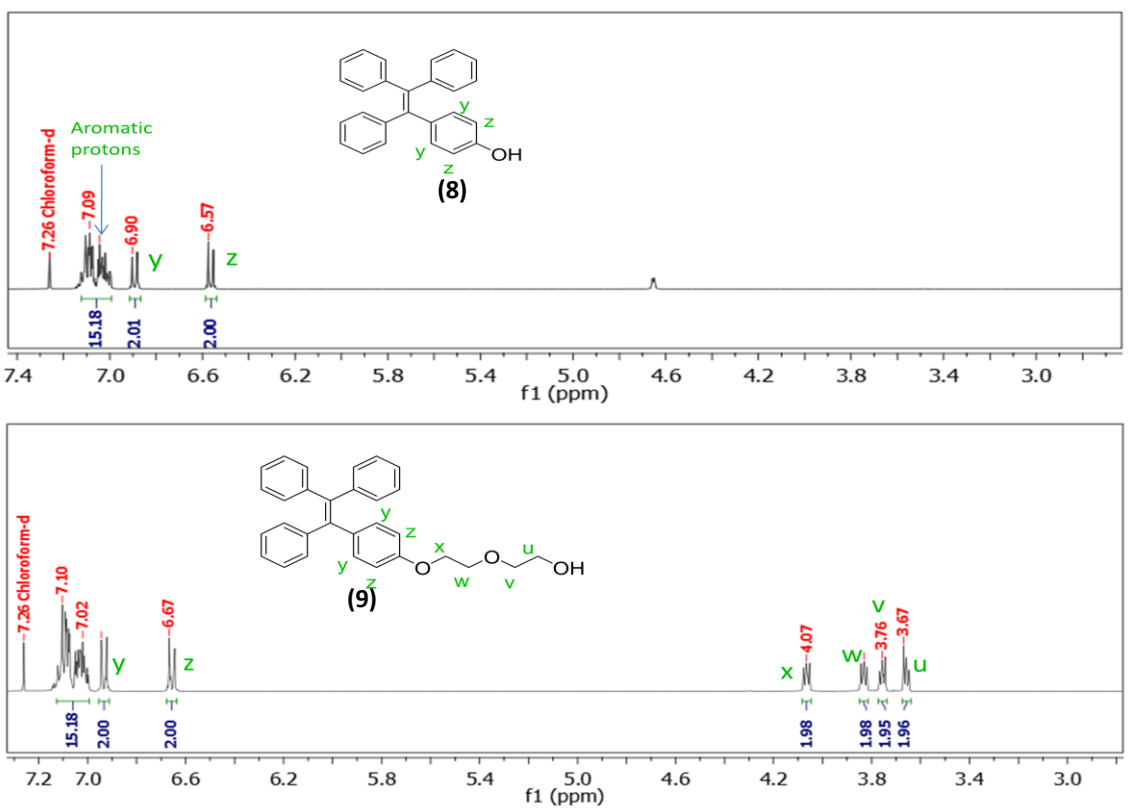

Figure 5.1: ^{1}H NMR for TPE initiator

BPCL monomer was synthesized by following the synthesis scheme 3.1. It was obtained by Baeyer villager oxidation of compound **2** and appearance of 4 ‘d’ protons at 4.47,4.03, 2.96 and 2.38 confirms the formation of compound (7).

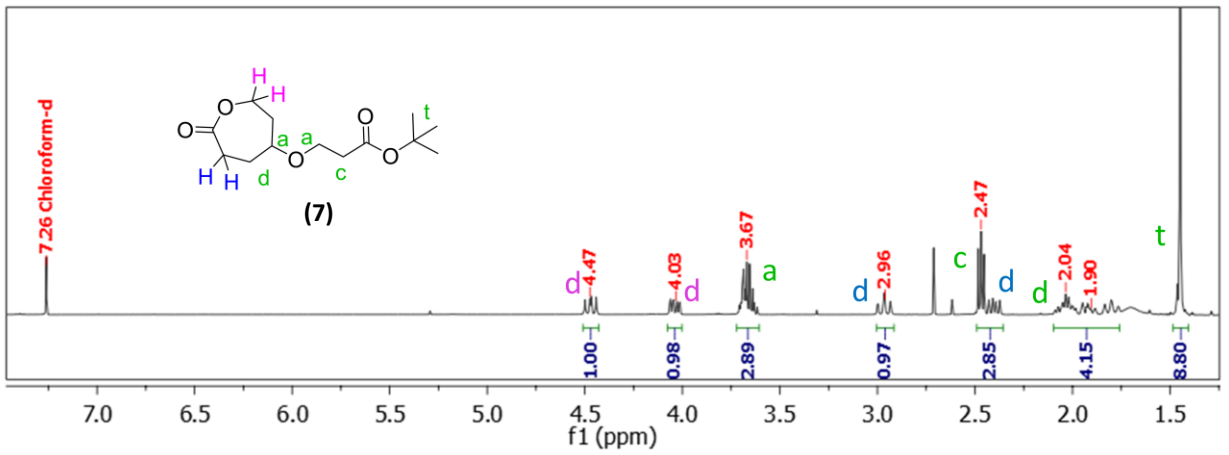

Figure 5.2: ^{1}H NMR for BPCL monomer

Using compound 9 as a initiator and compound 6 as a monomer an macro initiator (MI, 10) TPE-PPCL$_{10}$ was obtained via ROP. Giving integration of 2H to peak ‘z’, peak ‘c’,(correspons to PPCL) gives integartion of 10H and thus it confirms the formation of MI.

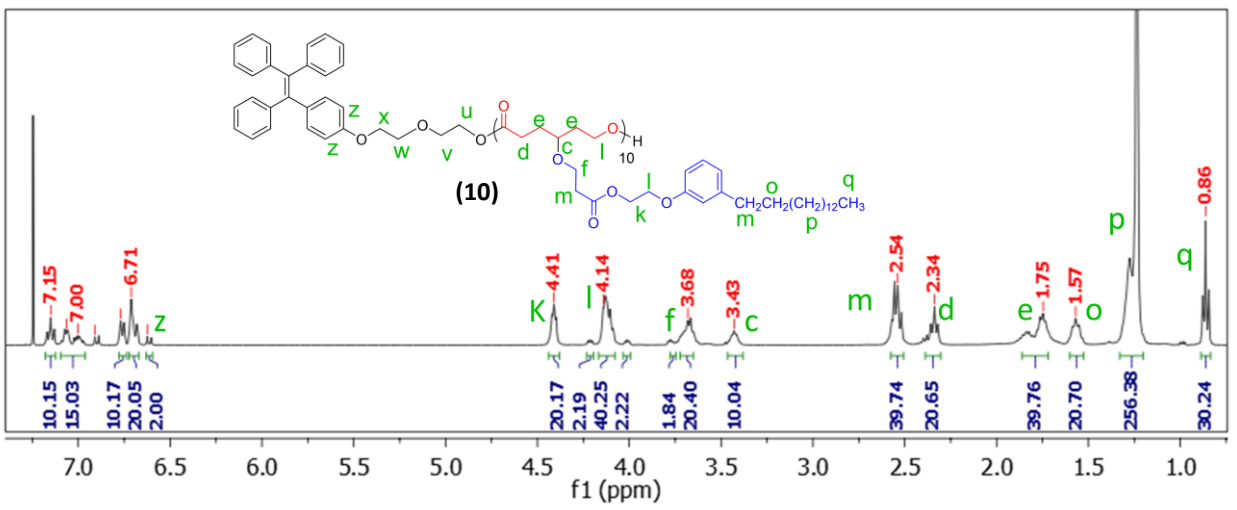

Figure 5.3: ^{1}H NMR for TPE-PPCL$_{10}$ (MI, 10)

MI (10) was further used to ring open the BPCL monomer to get TPE-PPCL$_{10}$-*b*-BPCL$_{50}$ (11), appearance of peak ‘t’ (spectra below)confirms the formation of polymer 11 and increase in the interation of peak ‘c’ to 59H from 10H (of MI) confirms the formation of polymer with desired number of repeating unit.

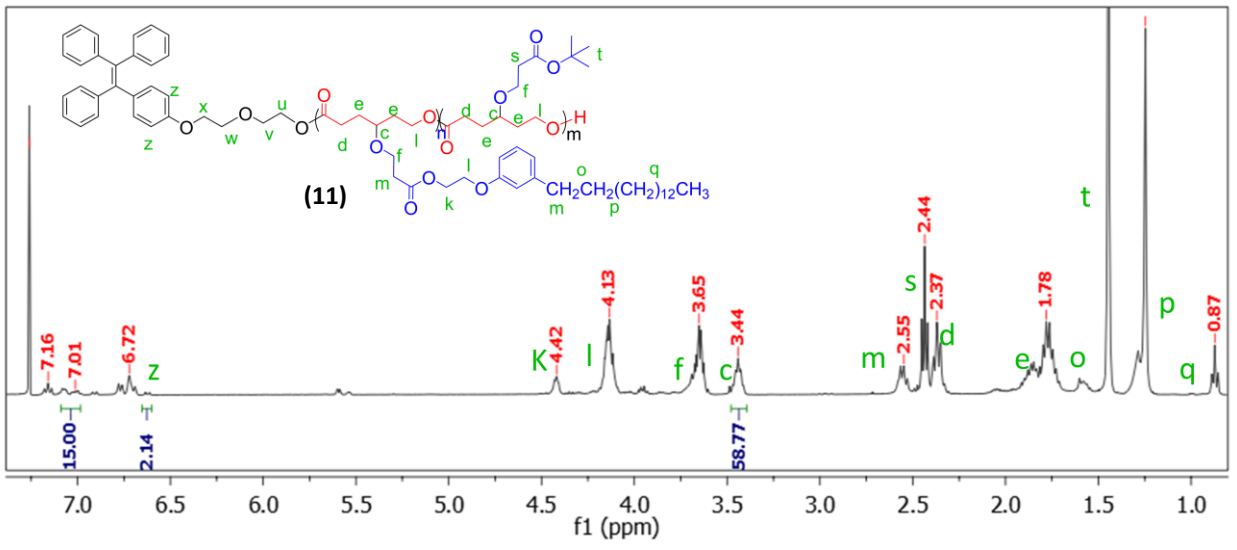

Figure 5.4: ^{1}H NMR for TPE-PPCL$_{10}$-BPCL$_{50}$ (11)

Polymer **11** was further deprotected using TFA to get amphiphillic polymer **12** and disappearance of peak ‘t’ (spectra below) confirms the formation.

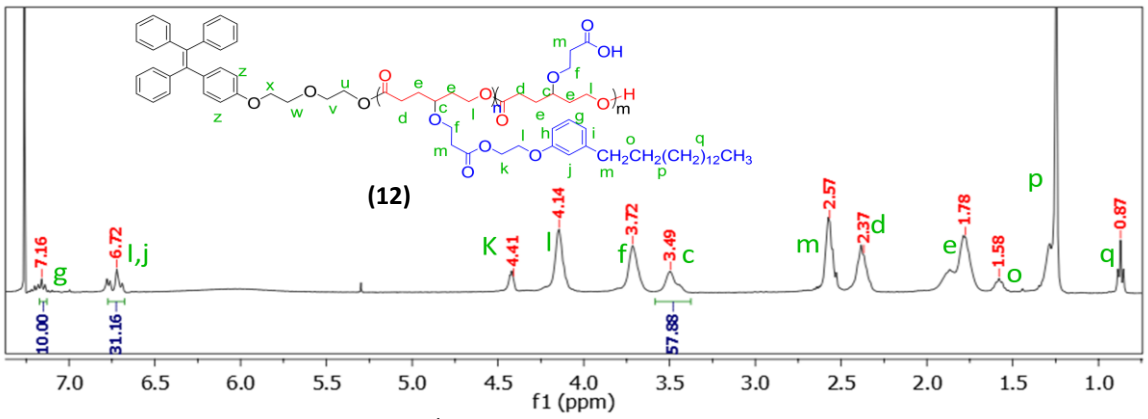

Figure 5.5: ^{1}H NMR for TPE-PPCL$_{10}$-CPCL$_{50}$ (12)

5.2 GPC, DSC and TGA Characterization of polymers:

Purity of all the polymers was reconfirmed by Gel Permeation Chromatography, monomodal distribution of all the polymers in figure 5.6 (a) led us to conclude that all the polymers are pure, we can see that polymer with highest Mw has been eluted first, broad intensity peak for TPE-PPCL$_{10}$-BPCL$_{50}$ suggests that the PDI for this polymer is high, it might have happened because it was synthesized from a macro-initiator (Scheme 5.1), which is also a polymer and thus adds into the polydispersity. Mw, Mn and polydispersity index (table 5.1) was also determined from GPC. Thermal stability was determined by TGA (Figure 5.6 (b)) and it was observed that polymers are stable up to 200 °C. Crystallinity of polymers was determined by doing differential Scanning Calorimetry (DSC), it is observed (figure 5.6 (c)) that all the polymers are semicrystalline in nature and crystallization temperature lies between 15-20 °C, which is lesser than that of polymer, TPE-PCL.

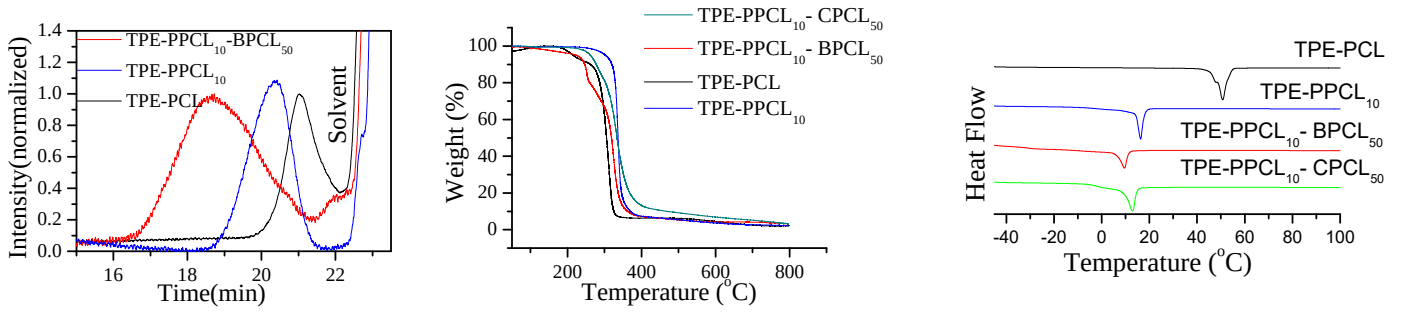

Figure 5.6: (a) GPC chromatogram (b) TGA thermograms (c) DSC thermograms

		NMR			GPC		
S. No.	Polymer	Feed (M/I)	Incorporated	Mn (g/mol)	Mn (g/mol)	Mw (g/mol)	PDI
1	TPE-PCL	50	49	6029	2000	2500	1.22
2	TPE-PPCL$_{10}$	10	10	5764	5000	7100	1.4
3	TPE-PPCL$_{10}$-BPCL$_{50}$	50	48	11471	15900	33400	2.09

Table 5.1: ^{1}H NMR and GPC Characterization of polymers

5.3 Self assembly of polymer, Rhodamine-B and Nile red encapsulation:

Self assembly studies (as explain in the methods) were performed to see whether these newly synthesized polymers are forming some nanostructures. Upon dialysis of nascent polymeric solution against water it was observed that dialyzed solution was clear and it forms nano-assemblies of the size 126±5nm.

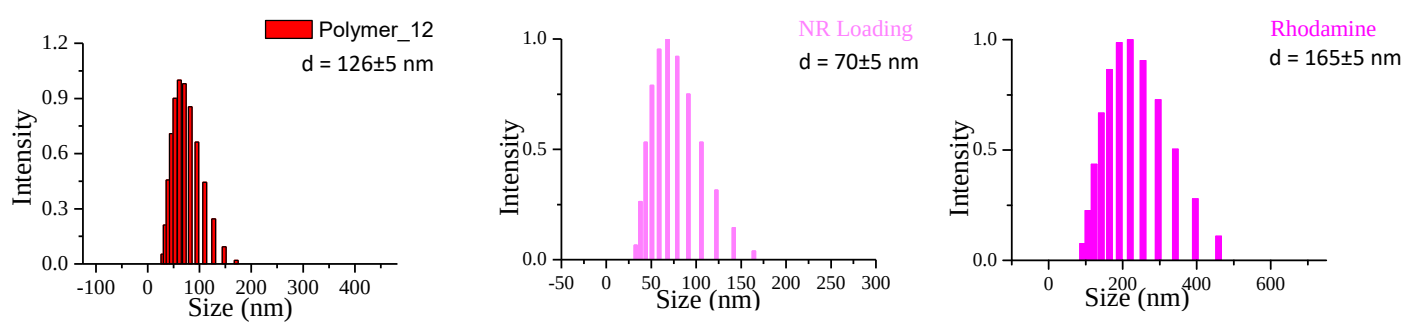

Figure 5.7. DLS histograms for polymer self assembly, Nile red and Rhodamine loaded nano-carriers

To check whether these are micellar or vesicular assemblies nile red and Rhodamine-B loading was carried out and it was observed that it could load both the dies and forms nano-assemblies with size 70 ± 5 nm and 165 ± 5 nm (Figure 5.7) respectively, thus we can conclude that these polymeric chains can self assemble into vesicular assemblies and can infer that, PDP substitution alone could not contribute for the formation of vesicular morphology, but as we used CPCL as a hydrophilic block instead of PEG, this polymer assembled into vesicles. DLC and DLE of Rhodamine-B loaded assemblies was obtained from the UV visible spectroscopy. It showed DLC = 0.45 % and DLE = 4.5 %. Further Doxorubicin loading was checked in these assemblies and it was found that, DLC of these polymers is higher than PEG-b-PPCL (DLC = 2.36 %) and thus we can say that TPE-PPCLn-CPCL polymers are more efficient and stable in drug loading than the later.

UV-Visible Spectra	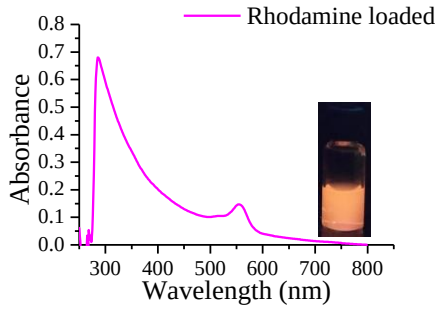	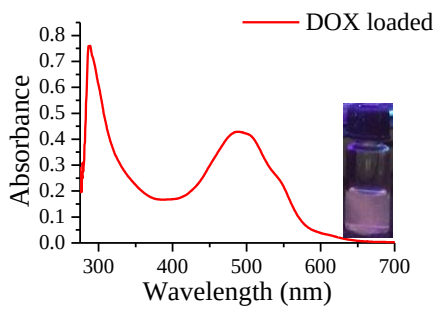
DLC (%)	0.45	4.25
DLE (%)	4.5	42.5

Table 5.2: Absorbance studies for Rhodamine loaded and DOX loaded nanocarriers

5.4 Photophysical studies:

We have incorporated fluorescent TPE molecule into the polymers so that, they can be used for bio-imaging purpose, thus it is necessary to see how these polymers behave upon interaction with light. TPE is a flurophore, which shows aggregation induced emission, this happens because when individual molecules are there in the excited state the phenyl ring rotates freely and this rotation leads to energy decay in a nonradiative manner, but once these molecules aggregate these intramolecular rotations are restricted and this leads to blocking of nonradiative decay and undergoes radiative decay.

By using TPE as an initiator and attaching it to the one end hydrophobic block, we are expecting that, when these polymeric chains will self assemble TPE molecules will aggregate into the hydrophobic part, shown in Figure 5.8(a) and this aggregate will lead to fluorescence or radiative decay. To check this hypothesis we obtain the fluorescence spectra (Figure 5.8 (b)) of dialyzed solution of nascent polymer (OD = 0.7) by exiting it at 330 nm and as we can see in the spectra emission peak at 445 nm (corresponds to aggregated TPE) is observed, which confirms that TPE has indeed aggregate in the hydrophobic shells of the nano-assemblies.

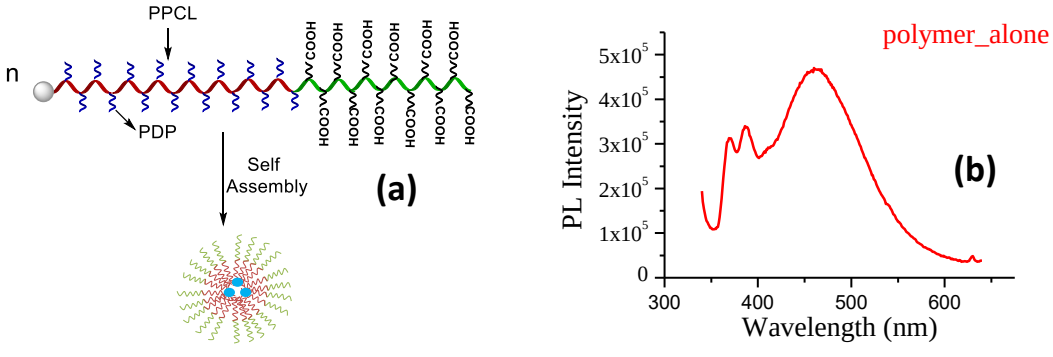

Figure 5.8: (a) Polymeric self assembly, which shows AIE, (b) absorbance spectra for polymeric self assembly

Further in our lab it has been shown that TPE and some other dies form FRET (Forster Resonance Energy Transfer) pair, where one molecule acts as a donor (D), which transfers its electronic energy to the acceptor (A) and due to this phenomenon one observes decrease in the emission of D and emission due acceptor molecule when the system is excited at λ_{max} of donor molecule. There are two necessary conditions for this phenomenon to occur, that is, D and A should have overlapping emission spectra and absorption spectra respectively and second is, both of them should lie close to each other such that their distance is in the range of forster distance (varies for each FRET pair). To validate the concept of FRET, Rhodamine-B loaded nano-assemblies were radiated with light of 330-340 nm (λ_{max} for TPE) range and it was observed that, there is a decrease in the emission of TPE (Poly_alone in the plot) and emission of Rhodamine-B at 580 nm (Rh_loaded in the plot) was observed, which is lower than the emission intensity of Rhodamine (Rh in the plot, when excited at 480 nm, λ_{max} of rhodamine) but higher than the residual intensity of Rhodamine (Residual Rh, when excited at λ_{max} of TPE) and this suggests that the FRET is happening.

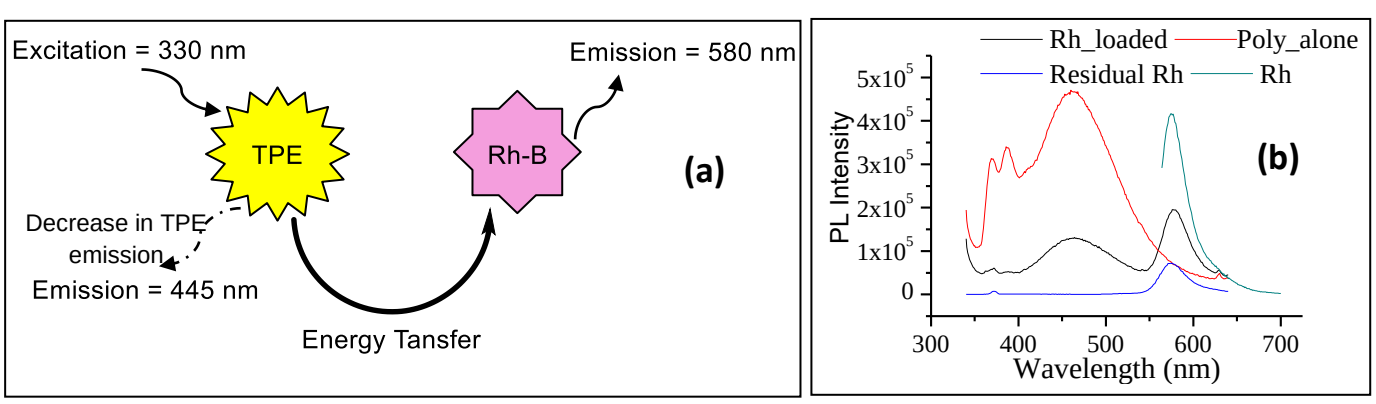

Figure 5.9: (a) Pictorial representation of FRET (b) Comparison of Fluorescence spectra to show FRET

5.5 Conclusion:

Carboxylic group functionalized amphiphillic block copolymers with TPE as a initiator were successfully synthesized via ROP, further it was found that, these polymers can self assemble into vesicular nano-assemblies, which are fluoroscent due to aggregation of TPE (shows AIE) molecule in the hydrophobic shell. Photophysical studies of Rhodamine-B loaded nanocarrier showed that TPE and encapsulated Rhodamine forms a FRET pair and FRET is observed.

5.6 Future Directions:

- Study the photo physics and cellular uptake of DOX loaded nanocarriers.
- Synthesize polymers with different size of hydrophilic block (CPCL) and see its effect on self assembly.
- Synthesize polymers with TPE attach to the hydrophilic end of the block copolymer (as shown in the scheme 5.2) and study the Photophysical properties of their self assemblies.

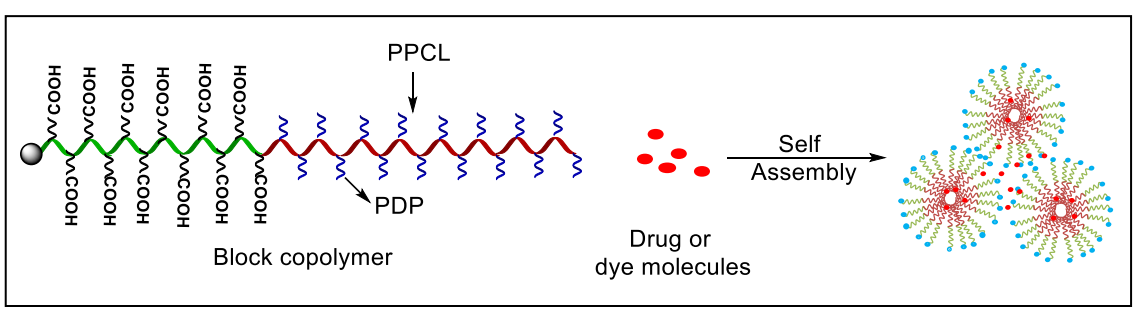

Scheme 5.2:

References:

1. Hardenia, A.; Tekade, R.K.; Maheshwari, N.; Hardenia, S. S.; Dwivedi, S. K.; MAheshwari, R. Scientific Rationale for Designing Controlled Drug Delivery Systems
2. Dechy-Cabaret, O.; Martin-Vaca, B.; Bourissou, B. Controlled Ring-Opening Polymerization of Lactide and Glycolide. Chem. Rev. **2004,** *104*, 6147-6176
3. Ge, Z.; Liu, S. Functional block copolymer assemblies responsive to tumor and intracellular microenvironments for site-specific drug delivery and enhanced imaging performance. *Chem. Soc. Rev.,* **2013**, *42*, 7289-7325
4. Feng, H.; Lu, X.; Wang, W.; Kang, N-G.; Mays, J. Block copolymers: synthesis, self-assembly and applications. *Polymers.* **2017**, *494*, 500-432
5. Yu, Y.; Chen, C-K.; Law, W-C.; Mok, J. Zou, J.;Prasad, P. N.; Cheng, C. Well-Defined Degradable Brush Polymer−Drug Conjugates for Sustained Delivery of Paclitaxel. Mol. Pharmaceutics **2013**, *10*, 867−874
6. Genevieve, G.; Dufresna, M-H.; Vinayak, S.; Ning, K; Dusica, M.; Jean, L. Block copolymer Micelles: preparation characterization and application in drug delivery. Journal of controlled release. **2005**, *109*, 169-188
7. Hong, C-Y.; Pan, C-Y. Direct Synthesis of Biotinylated Stimuli-Responsive Polymer and Diblock Copolymer by RAFT Polymerization Using Biotinylated Trithiocarbonate as RAFT Agent Macromolecules **2006,** *39,* 3517-3524
8. Rainbolt, E. A.; Washington, K. E.; Biewer, M.C.; Stefan, M.C. Recent developments in micellar drug carriers featuring substituted poly(ε-caprolactone)s. Polym. Chem., **2015**, *6*, 2369–2381
9. Kim, J. K; Yang, S. Y.; Lee, Y.; Kim, Y. Functional nanomaterials based on block copolymer self assembly. Progress in Polymer Science. **2010**, *35,* 1325–1349.
10. Mai, Y.;Eisenberg, A. Self assembly of block copolymers. Chem. Soc. Rev., **2012**, *41*, 5969–5985
11. Bates, F. S.; Fredrickson, G. H. Block Copolymers—Designer Soft Materials Phys. Today. *1999*, *52(2)*, 32-38
12. Labet, M.; Thielemans, W. Synthesis of polycaprolactone: a review. Chem. Soc. Rev. **2009**, *38*, 3484–3504.
13. Woodruff, M. A.; Hutmacher, D. W. The return of a forgotten polymer—Polycaprolactone in the 21st century. Progress in Polymer Science. **2010**, *35,* 1217–1256.
14. Malhotra, M.; Surnar, B.; Jayakannan, M. Polymer Topology Driven Enzymatic Biodegradation in Polycaprolactone Block and Random Copolymer Architectures. Macromolecules **2016**, *49*, 8098−8112.
15. Surnar, B.; Subash, P. P.; Jayakannan, M. Biodegradable Block Copolymer Scaffolds for Loading and Delivering Cisplatin Anticancer Drug. *Z.* Anorg. Allg. Chem*.* **2014**, *640, (6),* 1119–1126
16. Surnar, B.; Jayakannan, M. Stimuli-Responsive Poly(caprolactone) Vesicles for Dual drug Delivery under the Gastrointestinal Tract. *Biomacromolecules* **2013**, *14,* 4377-4387.
17. Pramod, P. S.; Takamura, K.; Chaphekar, S.; Balasubramanian, N.; Jayakannan, M. Dextran Vesicular Carriers for Dual Encapsulation of Hydrophilic and Hydrophobic Molecules and Delivery into Cells. *Biomacromolecules* **2013**, *13,* 3627-3640.
18. Kashyap, S.; Jayakannan, M. Amphiphilic Diblocks Sorting into Multivesicular Bodies and Their Fluorophore Encapsulation Capabilities. J. Phys. Chem. B **2012**, *116*, 9820−9831
19. Surnar, B.; Jayakannan, M.; Sharma, K.; Core–shell polymer nanoparticles for prevention of GSH drug detoxification and cisplatin delivery to breast cancer cells. Nanoscale, **2015**, *7*, 17964-17979

20. Surnar, B.; Jayakannan, M. Structural Engineering of Biodegradable PCL Block Copolymer Nanoassemblies for Enzyme-Controlled Drug Delivery in Cancer Cells. ACS Biomater. Sci. Eng. **2016**, *2*, 1926−1941
21. Surnar, B.; Jayakannan, M. Triple Block Nanocarrier Platform for Synergistic Cancer Therapy of Antagonistic Drugs. Biomacromolecules **2016**, *17*, 4075−4085
22. Kulkarni, B.; Surnar, B.; Jayakannan, M. Dual Functional Nanocarrier for Cellular Imaging and Drug Delivery in Cancer Cells Based on π‑Conjugated Core and Biodegradable Polymer Arms. Biomacromolecules **2016**, *17*, 1004−1016
23. Kulkarni, B.; Jayakannan, M. Fluorescent-Tagged Biodegradable Polycaprolactone Block Copolymer FRET Probe for Intracellular Bioimaging in Cancer Cells. ACS Biomater. Sci. Eng. **2017**, *3*, 2185−2197